Design and Fabrication of a Powder Cleaning Apparatus for Additively Manufactured Complex Parts

A Major Qualifying Project submitted to the faculty of Worcester Polytechnic Institute in fulfillment of the requirements of the Degree of Bachelor of Science

Submitted By:
Eliana Abenante
Geoffrey Hadden
Nathan Johansen
Lucio Nicoletti

Submitted To:
Professor Sneha P. Narra, Advisor
Professor John Sullivan, Advisor

May 18, 2020

Abstract

Additive manufacturing, specifically metal powder bed fusion processes, have various applications in the medical, aerospace, energy, and automobile industries. However, there are still several challenges that need to be addressed in these manufacturing processes. Categorically, there is the problem of cleaning the parts after the process is completed. This is a crucial step as without proper removal, these powders can create a significant hazard during post processing processes and use. While there are several approaches to powder removal, there remains a need for a reliable technique that abides by safety limitations and constraints while also removes powder thoroughly. The goal of this project is to make a reliable and efficient system for loose powder removal for parts additively manufactured via powder bed fusion processes. To meet this goal, the project team focused their research on the fundamental issue of post fusion powder removal in a laser powder bed fusion (LPBF) process. A prototype apparatus was designed, analyzed, and constructed to remove residue powder from LPBF parts. Future testing can be done with this prototype to determine usability, efficiency, and compliance with required safety factors.

Acknowledgements

We would like to thank our advisors, Professor Sneha P. Narra and Professor John Sullivan, for their support and guidance throughout this project. We would also like to thank the staff of Washburn Labs, and in particular Ian Anderson and James Loiselle, for all of their help in working with us to bring our project to fruition.

Executive Summary

Additive Manufacturing (AM) is a rapidly growing form of manufacturing due to its many advantages over traditional manufacturing methods. It offers the possibility to produce parts that have complex and intricate features, that either would be too expensive, or impossible to produce with traditional manufacturing techniques. This aspect of AM allows for weight reduction and part consolidation. AM can be classified into two main subsets of processes: polymer/indirect metal, and direct metal. This project focuses on post-processing of parts produced via laser powder bed fusion process (LPBF) that falls under the direct metal AM category. Finished LPBF parts are embedded in metallic powder, and the first step of post processing these parts is to remove residual powder which is the project goal.

The beginning of our design process started with two potential solution concepts. One involved a pendulum-based system, powered by hydraulics. The pendulum would have a part mount at the bottom that would be rotated by a step motor. With the part rotation and pendulum, oscillation, the design aims to have gravity remove the powder with constant changes in the gravitational vector. The second initial design aimed to have the user control a compressed air gun to remove the powder. Our team advanced the pendulum design as feasible, albeit with modifications. This design went through several iterations, with most notably, the hydraulic motion was replaced with a motorized 4 bar linkage. The design was modeled in Creo to demonstrate functionality and validate part design selections. This computer aided design (CAD model) served as a blueprint for our prototype.

Our design was fully automated, with all motion powered by motors, and controlled by an Arduino. Incorporating an Arduino allows for easy change in parameters according to the user's specifications. The motors were all assembled with gear ratios to obtain a reliable mechanical advantage while allowing the use of small and cost-effective motors. The prototype incorporates a sealed environment with a detachable powder-catch bin.

The prototype was successfully assembled with all mechanisms running as designed. Next steps for this project would involve testing of the functionality of powder removal. Test parts were designed and modeled to incorporate a variety of part geometries that this apparatus is expected to clean in the future. Suggested testing procedures were compiled to find optimal parameters of the motors for different powder sizes and flowability.

List of Figures

List of Tables

Nomenclature

AM....Additive Manufacturing

DMD....Direct Metal Deposition

DMLS....Direct Metal Laser Sintering

EBM....Electron Beam Melting

FDM....Fused Deposition Modeling

HIP....Hot Isostatic Pressing

LAM....Laser Additive Manufacturing

LPBF....Laser Powder Bed Fusion

NFPA....National Fire Protection Agency

PBF....Powder Bed Fusion

PEL....Permissible Exposure Limit

SLS....Selective Laser Sintering

Table of Contents

1 Introduction

1.1 An Overview of Manufacturing

The definition of manufacturing or to manufacture is to convert raw materials, components, or parts into finished goods that meet a customer's expectation (Business Dictionary 2020). Developments over the past three hundred years has increased our ability to produce these goods at an increasingly rapid rate, improving the quality of life for many people around the world. Almost all the commodities that you may touch daily can be traced to a manufacturing plant somewhere around the world. For example, most smartphones are assembled in large factories in China, a luxury sedan car from Germany, or a Wilson football made in Ohio. These are just a few examples of items that are readily available for purchase, thanks to many key inventions from the past. Historians have categorized these periods of great technological advance into three to four industrial revolutions (Pouspourika 2019). These periods are separated based upon when the most important and iconic inventions were created.

1.2 The First Industrial Revolution

The first major advancement that led to an increase in production on a large scale was the invention of a steam engine. The first steam engine was developed and built by Thomas Savery in 1698 in order to aid the pumping of water from coal mines (Palermo 2014). The introduction of this technology started the transition of society from being predominantly dependent on farmers and craftsman to urbanization. The steam engine drove an industry wide change in the way that both machines and transportation methods were powered. To be more specific this included steam ships and trains which connected many isolated areas and decreased the effort to get from point-to-point. In terms of a specific manufacturing impact, the creation of the power loom by Edmund Cartwright reduced the need for human input, dramatically increasing output of the booming textiles industry (Vyas 2018). Finally, another hallmark of this era was the development of puddled iron by Henry Cort. This was a new process of stirring molten metal in a reverberatory furnace, allowing iron to increase its flexibility and reducing its tendency to shatter. This combination of a high-volume production method and a more reliable material led the way for iron to be used in more applications (Encyclopedia Britannica).

1.3 The Second Industrial Revolution

This next period focused on improving previous innovations and providing the world with the most important piece of technology, usable electricity. This time period can be categorized between the mid nineteenth to mid twentieth centuries. The most prominent inventions of this era were the telephone, the lightbulb, and the internal combustion engine. During this revolution, there was also a substantial increase in production of oil, steel, and electricity (Schulze 2019). The telegraph was invented by Samuel Morse in the 1800's, which was then superseded by Alexander Graham Bell's telephone which turned sound into an electrical signal through vibrations transmitted to a membrane. This process was then reversed on the receiving side to recreate the sound (How it Works 2012). This invention was the start of a communications revolution that turned transferring information from a laborious task into an on-demand service. Regarding manufacturing there were two critical technologies/processes that came from this era, the lightbulb and the assembly line. While Thomas Edison may not have been the initial inventor of the lightbulb, he was able to make it commercially viable. Many any people think that this invention is crucial due to its usability in the household, but it also allowed factories to be well lit at night, creating the opportunity to run continuously with multiple shifts of workers. The most innovative process shift in the manufacturing and the assembly line, was introduced to the world in 1913 by Henry Ford, aiding the production of the Model T automobile (History 2019). An assembly line is a series of specialized workers and machines in a factory by which a succession of identical items is progressively assembled. This revolutionary manufacturing technique cut down the time to build a single unit from over twelve hours to two and a half hours. By implementing this new process, it allowed the Ford company to produce fifteen million Model T's in just fifteen years (Vyas 2018). Assembly lines were then widely adopted across any and all industries that consisted of combining many individual parts into one final complex item for sale.

1.4 The Third and Fourth Industrial Revolutions

With each of the previous two revolutions, there has been a few specific technologies that have marked the beginning of one and the end of the other. With the third industrial revolution, the development separating it from the second was the development of the semiconductors, the computers, and the internet. The start of this period can be categorized as mid-twentieth century, finishing at the start of the twenty first. These developments led to further advancements such as programmable logic controllers, and robots which have helped automate production and, reducing the need for human labor (Sentryo 2017). All these developments have led to an increase in communication between those involved in the production of goods. These have since brought new principles of manufacturing such as five lean six sigma principles (Mehrjerdi, 2011). These are manufacturing techniques to maximize the efficiency of a production system by removing any waste or downtime between processes or assembly. These technologies have altered the way that we as humans interact with each other and have only been around for the past fifty years.

There is not a consensus as to if the fourth industrial revolution has begun because there is a blending of technologies. Many experts are leaning towards the idea that we are currently going through the shift between the two, due to the developments of artificial intelligences, the internet of things, genetic engineering, quantum computing, and arguably the most important for manufacturing; 3D printing (Xu 2018). The general process of 3D printing both plastics and metals has been around since the 1980's but has only recently entered limited production. Companies are beginning to design parts for this process rather than applying older designs to the new process (Herderick, 2015). This is crucial because with 3D printing, material can be deposited only where needed as opposed to previous casting techniques, reducing the amount of material used. Additionally, this new form of manufacturing reduces the time taken from design-to-prototype because of the ability of a part to be printed directly from a computer aided design file. These models can then be altered and reprinted to confirm any necessary changes without having to redesign tooling, molds, or fixtures. While 3D printing, also known as additive manufacturing, has may benefits, it also has many unique challenges depending on the process of interest. For laser powder bed fusion process, some of the challenges are associated with thermal stresses, need for support structures, requiring a powder removal step, and stress relief heat treatment before any additional machining can be performed.

1.5 Special Considerations due to Unforeseen events

This project team worked extensively and consistently for seven months on the project and was on the cusp of completion with the only objective left to complete being final testing of our apparatus. This was due to the COVID-19 global pandemic which prevented this project team from returning to campus in order to complete this final step. Our project team was able to test each individual component of our apparatus and the majority of them together. Nevertheless, our team is successful in the research, design, analysis, and construction of this project. We look forward to seeing the future developments this project initiated in years to come.

2 Background

2.1 What is additive manufacturing?

2.1.1 Additive Manufacturing 1987-2000

When starting the conversation about additive manufacturing, our team accepted the definition of "the process of joining materials to make objects from 3D model data, usually layer upon layer, as opposed to subtractive manufacturing methodologies" (Nanakoudis 2019). Additive manufacturing may seem like a relatively new buzzword in the field of manufacturing but is has been a commercial manufacturing technique since 1987 with the development of stereolithography (SLA) from 3D Systems (Wohlers 2016). This is a technique where ultraviolet (UV) light from a laser is used to cure a liquid polymer in specific areas to create an object. This UV selective curing process was an industry standard until 1990 when developments occurred to make these resins cure using visible light. In 1991, the technique of fused deposition modeling (FDM) was introduced by Statasys, this process heats a thermoplastic filament to its glass transition temperature and is then extruded through a tip one layer at a time to create a 3D object (Wohlers 2016). The next major development in this field came in 1992 from the company DTM, who were later bought by 3D Systems, in the form of Selective Laser Sintering (SLS). This new process used energy generated by a laser to fuse powder-based materials in a layer-by-layer pattern. The next breakthrough occurred in 1994 with the introduction of ModelMaker from Solidscape. This technique deposited wax-based materials using an inkjet print head and led to the ultimate decrease in the cost of 3D printers (Wohlers 2016). Prior to 1997, most additive manufacturing was limited to plastic-based polymers or thin sheets of laminated paper. However, a company by the name of AeroMet was founded and created the first laser additive manufacturing (LAM) process that utilized a high-power laser in order to melt titanium (Wohlers 2016). This was a breakthrough for the aerospace industry that required low weight and high strength components.

2.1.2 Additive Manufacturing 2000-Present

In the year 2000 a new process was developed by Precision Optical Manufacturing called direct metal deposition (DMD). This process utilized a system that fed metal powder through a nozzle that was then melted rather than on a powder bed like many systems use today (Wohlers 2016). The first developments for laser sintering as opposed to laser melting, which is fusing particles together rather than homogenously melting them together, occurred in 2001 from the company EOS Manufacturing Solutions. At this time, there were also developments in reducing the grain size of the powders used for these processes which ultimately increased the complexity of the designs these machines were able to manufacture. The first mention of direct metal laser sintering (DMLS) can be traced back to 2003 with the EOSINT M 270 which utilized a fiber-based laser rather than a CO_2 laser (Wohlers 2016). This process evolved to be known as laser powder bed fusion process (LPBF). Over the next few years, improvements were made to decreasing powder size, increasing the available materials, and decreasing the cost and size of 3D printers. This pattern continued for three years until 2006 when the first electron beam melting (EBM) systems were distributed in the united states. This is also known as electron beam powder bed fusion (E-PBF) process. The key difference between E-PBF and LPBF is the use of an electron beam rather than a laser. Both processes have their upsides with LPBF having the capability to use a broader range of materials, utilize a finer layer thickness, and generally result in a relatively smoother surface finish compared to E-PBF. E-PBF on the other hand has a lower level of internal defects and minimal residual stress due to high process temperatures (Park 2016). While these are two different styles of metal 3D printing, they can both be categorized as powder bed fusion manufacturing.

Many of the developments over the next half decade focused on a few main principles. The first was increasing the available material selection for additive manufacturing which significantly affected fields such as dental and biomedical where devices such as hearing aids were now able to be additively manufactured (Gibson, Rosen, & Stucker, 2010). Another principle that was focused on was reducing support waste and manufacturing time with many companies being able to reduce build structures by 40% and manufacturing time by 14% with the help of SMART supports by Stratasys (Wohlers 2016). The last big improvements were in the reduction of cost and space that these units cost. Many individuals could now own their own 3D printers which only furthered the applications of this relatively new manufacturing process. The next large processes-based development occurred in 2012 when Autodesk and Orgonovo Holdings first announced their collaboration to create a 3D printer for organic tissues (Wohlers 2016). Figure 1 demonstrates many of the significant developments over the past thirty years showing the increasing speed of the introduction of new technologies. These are the main additive technologies we see on the market today and they are poised to have an increasingly large impact on the way society both designs and manufactures parts.

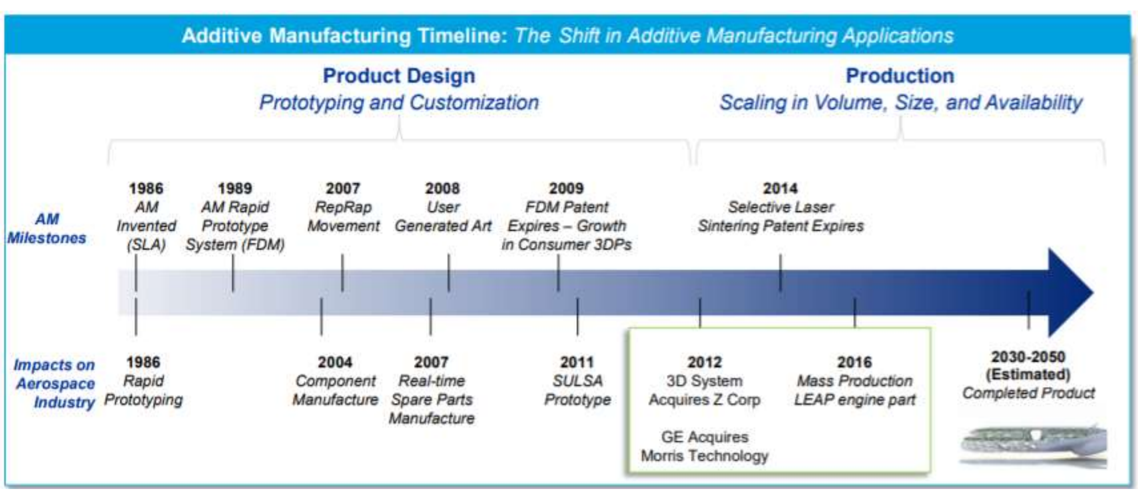

Figure 1: Timeline of Additive Manufacturing Developments (Cotteleer 2014)

2.2 Current Companies and Production Using PBF

Powder Bed Fusion (PBF) is currently being used in many different markets. Although it is a relatively new field in the manufacturing world, many companies are already utilizing the technique to create parts including Rolls-Royce, GE, NASA, General Motors, and Airbus. This is just a short list of a few large scale companies, however there are many uses and applications for additive manufacturing and companies are finding new ways to utilize this new technique.

Rolls-Royce is a British luxury company that manufactures and distributes products for the automotive and aviation industries. They have invested in additive manufacturing to develop aerospace parts. In 2015, Rolls-Royce flew the largest 3D printed aerospace component ever developed powering the Trent XWB-97 engine ("Rolls-Royce to Fly Large 3D Printed Part - 3D Printing Industry"). A direct competitor of Rolls-Royce, GE, has also been involved heavily in additive manufacturing by opening a massive additive manufacturing facility. This facility produces fuel nozzles for the LEAP jet engines (Anusci, "GE's Additive Technology Center in Ohio Uses 90 Metal 3D Printers to Make Aircraft Parts").

NASA also has a hand in the world of additive manufacturing. The metallic technique most used is powder-bed fusion or selective laser melting (SLM). These techniques have been used to combustion devices component hardware, liquid rocket engine components, and rocket engine nozzles that operate in extreme temperatures and pressures (Gradl, 2018). These are usually incredibly expensive and complicated to manufacture, but with additive manufacturing techniques, costs can be reduced, and development time can be cut.

General Motors (GM) has made headway in the automotive industry with additive manufacturing. In May of 2018, GM entered a "multiyear" Autodesk to create a "proof-of-concept, 3D-printed seat bracket that was 40 percent lighter and 20 percent stronger than the original part." ("GM's Use of 3D Printing Predicts Cheaper, Better Cars | WIRED", 2018) This bracket turned what had been an eight-piece assemble into a single component.

Airbus uses additive manufacturing for the purposes of weight reduction. Every kilogram saved in the design process can inhibit 25 tons of carbon dioxide emissions an aircraft gives off. Airbus is moving 3D printing technology into serial production. In 2017, the first titanium 3D-printed part was installed on a serial production aircraft which is a step forward in bringing more additively manufactured parts into production ("First Titanium 3D-Printed Part Installed into Serial Production Aircraft - Commercial Aircraft - Airbus", 2017).

2.2.2 Limitations

Although there are many advantages in using additive manufacturing techniques, such as reduced development time and design feasibility, there are still many limitations to using AM in serial production. One such limitation is the gap of knowledge of how to design parts for additive manufacturing. The process of 3D printing parts is still relatively new, and it requires a different design processes than other types of manufacturing that needs to catch up with the current technology ("Additive Manufacturing: Overcoming Current Limitations.", 2018) Another limitation is production costs. Although additive manufacturing does reduce the cost of design and development of a small subset of products, widespread adoption is not yet economically feasible.

As of now, traditional molding and machining is more cost effective than additive manufacturing for most products. This problem also falls in line with another limitation, which is production scale. Additive manufacturing machinery is primarily used for prototyping and not serial production. The machinery is also expensive, and it is not within most companies' abilities to use these on a large scale ("Additive Manufacturing: Overcoming Current Limitations.", 2018).

2.3 Process-Specific Issues

The main difference between E-PBF and LPBF is that the E-PBF uses an electron beam rather than a laser to melt the metal powder.

According to one of our survey respondents, who has worked as a manufacturing engineer for the past five years, the removal of the residual powder that remains attached to the metal piece differs between DLMS and E-PBF (Appendix A). DLMS produces a more powder-based residue that lends itself to be easily removed via a brush and non-static vacuum after separating and storing the metal piece in a sealed container. On the contrary, E-PBF produces a sinters a cake of powder, which attaches itself to the metal piece. The caked powdered must be chiseled away at within the E-PBF, which allows the residue to be reused for future processing. The remainder residue can then be removed by brush or another small utensil. Though their processes of left-over metal residue removal differ, both require attention and care to avoid contamination of the products and the manufacturing tools.

The challenges that are faced with additive manufacturing are mainly the fabrication of the piece itself, and the cleaning process to remove the left-over powder. E-PBF is very different from LPBF because they both have different design constraints and cleaning processes.

2.4 Comparing Powder Bed Fusion Materials

The adhesion between the particles depends highly on the atomic structure of the metal powder. In the process of powder bed fusion, you can use up to nine different types of metals, Stainless Steel 17-4 PH, Stainless Steel 316L, Aluminum AlSi10Mg, Nickle Alloy 625, Nickle Alloy 718, Titanium Ti64, Cobalt Chrome CoCrMo, MONEL K500 (age-hardenable nickel-copper alloy), and Copper C18150. The adhesion between these metals also depends highly on the application you want to use the part for. Depending on the application, you may want a metal that has excellent electrical conductivity, or a metal that has great corrosion resistance. For example, Stainless Steel 17-4 PH, is great for parts in the oil and gas industry, high ductility, strength, and parts requiring high corrosion resistance. While Aluminum AlSi10Mg, on the other hand is a very good powder for making thin complex walls at a cheaper price. Depending on the metal, there are many more benefits such as high heat application, good at welding, light weight, good thermal properties, and many more. (Stratasys, 2019) So, depending on the type of metal powder you want to mold depends highly on what the application you want to use that metal for.

Table 1. List of Materials used in Additive Manufacturing (Stratasys, 2019)

Material	Composition	Application
Stainless Steel 17-4 PH	Martensitic, Chromium-Nickel-Copper Precipitation-Hardening	• Oil and Gas Industry • Ductile and High Strength • High Corrosion Resistance • Post-Production Processing
Stainless Steel 316L	Austenitic Stainless Steel	• Oil and Gas Industry • Ductile and High Strength • High Corrosion Resistance • Post-Production Processing • Consumer/Automotive/ Aerospace
Aluminum AlSi10Mg	Casting Grade Alloy	• Low Weight • Good Thermal Properties • High Strength and Hardness • Fast Building • Excellent Machinability
Nickel Alloy 625	Nickel Based Superalloy	• High Heat Applications • Turbine Engine and Fuel System Components • Used in Oil, Petroleum, and Natural Gas Industry • Non-Magnetic
Nickel Alloy 718	Nickel Based Superalloy	• Non-Magnetic • Corrosion Resistant • High Heat Applications

		• Turbine Engine and Fuel System Components • Used in Oil, Petroleum, and Natural Gas Industry
Titanium Ti64	Alpha-beta Titanium Alloy	• Excellent Mechanical properties for High Performance Engineering Applications • Corrosion Resistant • Low Specific Weight • Biocompatibility
Cobalt Chrome CoCrMo	Metal Alloy of Cobalt and Chromium	• Dental Restorations
MONEL K500	Age-harden able Nickel-Copper Alloy	• Corrosion Resistant • Liquid Rocket Components • High Ductility and Strength • LOX Manifolds and Injectors
Copper C18150 (CuCr1Zr)	Chromium Zirconium Copper Alloy	• Excellent Thermal and Electrical Conductivity • Plastic Mold Components • Induction Coils • Regeneratively Cooled Nozzles

2.5 Challenges with Powder Bed Fusion

Powder bed fusion proposes two groups of challenges as a method of manufacturing. There are issues that arrive in the nature of the process such as the thermal stresses involved in the process or the need for support structures, and then there are hazards to the operators of these machines. Though operating the powder bed fusion machinery, itself poses several hazards, the most critical repercussions involve occupational exposure to fine metal powders at different stages in the process including the post process cleaning. These metal powders have combustible properties and are highly toxic when inhaled. An understanding of what to be cautious of while working with fine metal powders allows proper decisions to be made concerning cleaning parts following post-processing.

2.5.1 Thermal Stresses

One of the first major issues with powder bed fusion, especially regarding metal sintering versus electron beam melting, is the residual stress in a part due to the rapid heating and cooling of thin layers of powder. Once metal is heated, it will immediately start to cool and contract once the small area of the laser has move to a different position. Once the laser returns to the previous position to melt a new layer, it will not only melt the top layer, but will reheat the previous layer cause it to then expand and contract an additional time (Roehling 2019). This process will continue with multiple layers until the energy of the laser or electron beam reaches its maximum penetration depth. Generally, this heating and cooling will cause a compressive stress towards the center of a part and a tensile stress towards the edges of a part due to them cooling the fastest whereas the edges are going to be pulled inwards. (Roehling 2019) While this is a general assumption there can be a large variance in the type and location of these residual stresses due to many factors such as metal type, grain size, preheat temperature, and strength of laser (Li 2018). The reason that this is more apparent in laser sintering, as opposed to melting, is that most electron beam melting processes will preheat the metal powder to reduce the temperature gradient (Li 2018). These large thermal stresses can lead to distortions and cracks in the part if not properly dealt with. Additionally, these distortions may not be visible to a human eye and could go undetected, ultimately causing a failure in the part or assembly leading to a significant risk to the end user. While our project scope is not about the thermal stresses associated with powder bed fusion, it is important to note that all residue powder must be removed before any post process annealing takes place due to the need to cut the parts from the base plate, and removal of any support structures. This cutting process has the potential to create sparks which can ignite the residual powder cause a danger for the operator preforming this step.

2.5.2 Support Structures

During powder bed fusion manufacturing, support structures are utilized to the ensure the part is made correctly. Main problems where they are needed include parts with curvatures and overhanging features. Without support structures, more extensive post processing would be required. Support structures come in a variety of options depending on the situation and come with different benefits and difficulties. The two types of support structures are called active and passive. Active supports are more common. These supports are used for material that is overhanging or at an angle that the machinery can’t handle. One problem that these support structures have is that they become connected to the part after the process. This causes an optimization problem between parts being strong enough to support the part while its being made versus structures that are too hard to be taken off the part during post-processing. The specific kinds of active support structures and their issues are well documented. (Morgan 2017)

One strategy is using thin-wall supports. These supports are prone to warping due to heating and cooling during manufacturing. These supports need to be designed such that they sturdily connected to the base plate. An alternate support type is grid supports. These supports are utilized during manufacturing of parts with large curvatures. It connects to several small points around the part to create support with minimal contact to the part. However, due to their thin nature, uneven powder density can cause material build up and make uneven layers. The third type of supports are solid supports. This is when the laser or beam passes horizontally in lines across the part. With this type of support, if the fabrication bead size deviates significantly, it can cause the layers to develop unevenly. A third type of support is full supports. This is used commonly for large and flat parts. Full supports are similar to hatching, but they connect to the base plate. This is an effective support but are they are only beneficial for specific situations (Morgan 2017).

2.5.3 Flammable Powders and Fire Risks

Many metal materials used for powder bed fusion are combustible and therefore explosive as dusts. While the degree of combustibility of each material is dependent on the amount of dust and the conditions of the environment, they all pose a risk of explosion. This sort of explosion can be caused by a spark, open fire, overheated surface, or an electrical discharge. The National Fire Protection Association (NFPA) has standards and regulations that have the purpose of reducing combustible hazards of dust. According to NFPA-484, the most particularly flammable metal powders used are aluminum, magnesium, titanium, tantalum, niobium, zirconium, and alloys of all these metals as well. Taking the dangers of flammable powders into account, it is important to take measure to reduce the risk of combustion in whatever type of cleaning apparatus we design. It is important for it to be a completely enclosed space with an inert environment, filled with nitrogen and not oxygen. NFPA-484 also outlines regulations on how to discard of combustible materials and how to control and extinguish these types of fires. Other protective measures should also be taken, including removing ignition sources, keeping work areas clear of dust accumulations, use spark resistant tools, and have satisfactory ventilation and fire suppression systems ("NFPA 484: Standard for Combustible Metals").

2.5.4 Toxic Properties of Powders

Fine metal powder can also have toxic properties when inhaled. In the industry of additive manufacturing, the average particle size of metal powder is 25 to 150 micrometers. Long exposure to these powders can reach toxic levels since the body cannot metabolize them. If the amount of powder a worker is exposed to exceeds the body's ability to excrete it, the excess can be deposited to various tissues in the body and can lead to various problems such as lung disease (Hamzah, 2016). For example, one big concern in terms of toxicity in additive manufacturing comes from exposure to cobalt. Cobalt is known to be neurotoxic, cause cancer, and cause several different lung complications. A study was done on toxic metal exposure titles "Metal dust exposure and lung function deterioration among steel workers: an exposure-response relationship." This study found that when steel workers were exposed to cobalt and chromium 1-3 times higher than the permissible exposure limit (PEL), there was an exposure-response relationship of cumulative metal dust exposure with the deterioration of lung function values. This meant that proper and efficient use of protection equipment was essential to maintain lung and respiratory health (Hamzah, 2016). Although these works experienced long-term exposure in a way that a worker in additive manufacturing would not, it still rises the concern of inhaling toxic metal particles in an enclosed environment. In the article titled "Safety and Workflow Considerations for Modern Metal Additive Manufacturing Facilities", the proper safety procedures for dealing with metal powder are outlined. These include the use of full-face respirators, segregating all equipment dealing with the powder to separate rooms with appropriate signage and access controls to prevent exposure for non-operators, and using anti-static vacuum cleaners to evacuate spilled powder (Scime, 2018). It is also important to have sticky-rooms to help clean off personnel that encounter the powder, and out keep all powder out of the drains. It is important to know how toxic powder can affect operators and proper prevention of exposure when designing the part-cleaning apparatus and consider how and where it will be used (Scime, 2018).

2.6 Current powder cleaning processes

2.6.1 Cleaning issues with additive manufactured parts

The powder bed fusion (PBF) processes have advanced significantly and have a myriad of advantages over other manufacturing methods. However, PBF process do have unique problems that need further investigation. Post-processing carries the most room for improvement. During PBF, parts are formed in beds of powder, which results in a finished part embedded in powder (Dassault Systemes 2019). Cleaning this powder completely off the part can prove to be an increasingly difficult, as a part becomes more complex. Leftover powder can be categorized by three different circumstances: unfused powder, trapped unfused powder, and half-fused powder. Unfused powder is simply the leftover powder that is the most easily removed using a brush. Trapped powder is the powder that becomes stuck on or in the part due to complex part geometry. Hollow spaces in intricate geometries and lattices are common examples of part geometry that trap powder (Dong 2019). Half-fused powder is the result when the PBF processes themselves cause powder to adhere on the part. During the forming process, the powder that is along the part geometry can and will be partially exposed to the laser or electron beam. This will result in powder that is half fused on to the finished part, which is more difficult to remove than loose powder (Tan 2017).

2.6.2 Standard cleaning procedures

There are methods to deal with this powder problem. However, none of them are perfect, and this area of post-processing requires further attention. Lot of the powder cleaning is done manually. Initially, the part is cleaned with a brush, aiming to remove all the loose powder it can. After the bulk is removed, leftover unfused and trapped powder are to be removed. This is done with compressed air (Dassault Systemes 2019). This is good for the powder that is stuck in semi-complex part geometry. Another technique that is utilized often is blasting which is done with sand, zirconia, alumina, or the identical metal as the part. Grains of the material are shot at the surfaces of the part, and these blasts are effective for dislodging powder (Bonini 2016).

2.6.3 Advanced cleaning techniques

One of the more advanced methods involve ultrasonic cleaning, depicted in Fig. 2 below. Ultrasonic cleaning can be done several ways depending on what the cleaning goals are. Using liquid mediums is a common practice, such as acetone, dilute water, and isopropanol. This is an effective method for cleaning most of leftover trapped and half-fused powder (Dong 2019). This is because of cavitation, which occurs during ultrasonic cleaning. Cavitation refers to the creation and the collapsing of bubbles when sinusoidal pressure is applied to a liquid. These bubbles release high velocity micro jets when they pop near solids. When this happens near the surface of the part, the micro jets efficiently dislodge powder. This cavitation can be made more abrasive to remove the half-fused powder. This is done by adding micro particles to augment cavitation (Tan 2017).

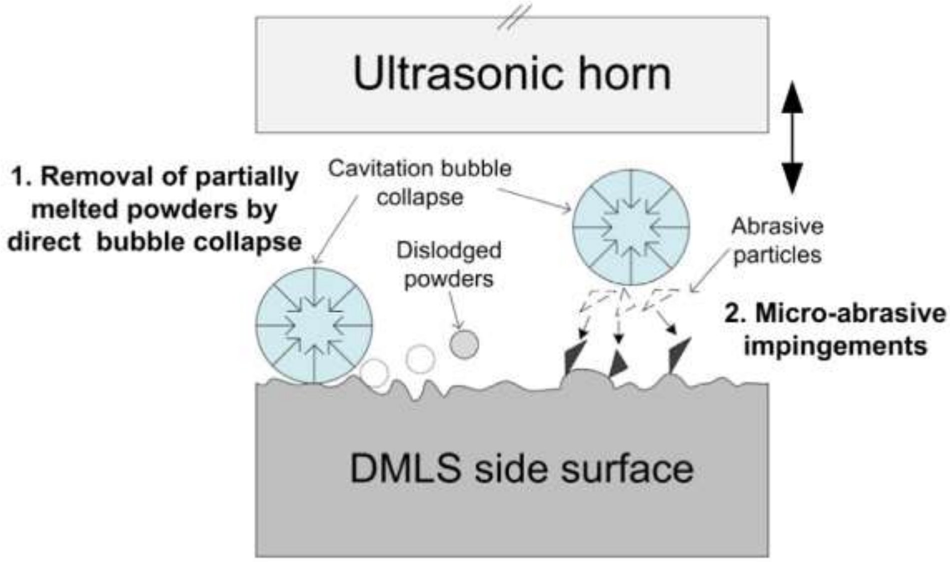

Figure 2: Ultrasonic Cleaning with Liquid Medium Tan, K., & Yeo, S. (2017)

2.7 Goals and Constraints

The goal of this project is to design a safe and efficient cleaning apparatus for powder bed fusion manufactured parts. Specifically, this cleaning process will be used to remove unfused powder and partially trapped powder within the part. The apparatus will be confined by specific functional constraints as outlined in next sections. One constraint is that the mechanism will exist in a sealed inert environment with no oxygen to avoid the possibility of combustion. This will also seal in toxic powder from contaminating any other surfaces. The cleaning process must also be successful in removing all unfused and trapped powder within the part before other steps in post-processing can be performed, since removing the part from its base has the potential to produce sparks that could ignite residual powder. In addition to the safety factors, our team also must estimate the durability of our design so that this apparatus can be used many times without the need for servicing or repair. There are also several design constraints for this device. It will need to be able to support roughly twenty pounds of weight from the part plus the base. Additionally, the containment unit need to be large enough to fit the manufacturing base from the printing process, as well as the length of arm connecting the structure to the frame. This apparatus will also have to have a wide enough base and an appropriate center of gravity to ensure it does not tip over. Our apparatus will also require a sealed containment unit to collect all of the powder for refusal. Finally, this project team will be powering this apparatus via multiple stepper motors so a force analysis to determine an appropriate motor must be completed. Since the project is going to be focused on cleaning one type of material, it does not have to be easily cleanable.

Table 2. Comparing Mechanical and Fluid Designs

Constraints	Mechanical Design	Fluid Design
Sealed Workspace	Y	Y
Pressurized	Y	N
Computer Automated	Y	N
User Access	N	Y
Inert Environment	Y	N
Motors	Y	N
Vacuum	Y	Y
Compressed Inert Gas	N	Y
Filtration	Y	Y
Part Moved During Cleaning	Y	N
Brush Piece	N	Y

3. Methodology

The goal of this project is to create an efficient and safe mechanical cleaning apparatus to facilitate powder removal from parts made through powder bed fusion. To accomplish this goal, the project was split into three components.

- The design process, which consists of determining the constraints of the project, establishing a design, and working out the amount/ type of loading the apparatus will be subject to.
- The building process, consisting of material selection and construction.
- The testing process to determine how to fully assess the apparatus and ascertain which results are needed to record the efficiency of the machine.

3.1 Design Process

The process of designing this cleaning device began with evaluating the constraints of the project and choosing among feasible designs to implement. After establishing a basic design for the mechanism, the loads and stresses were found for each essential piece of the device to determine how they can be made and what material they can be made from. Calculations were used to determine what types of motors would be required for the crank and the plate. Digital models were made of the design and adapted as pieces of the mechanism were changed.

3.1.1 Constraints and Initial Designs

The first step in the design procedure was determining the functional and design constraints that would restrict the scope of the project and provide limitations and expectations for the design of the apparatus. Functional constraints included safety measures and precautions. The workplace needed to be completely sealed and in an inert environment to avoid combustion of the powder. All the powder had to be kept contained so that other surfaces would not be contaminated and there would be no opportunity to breathe in the powder. Design constraints included the loads the mechanism would be subject to regardless of design, such as the weight of the base plate. Two initial designs were developed at the beginning - a purely mechanical design and a fluid design, as seen in Fig. 3 and Fig. 4.

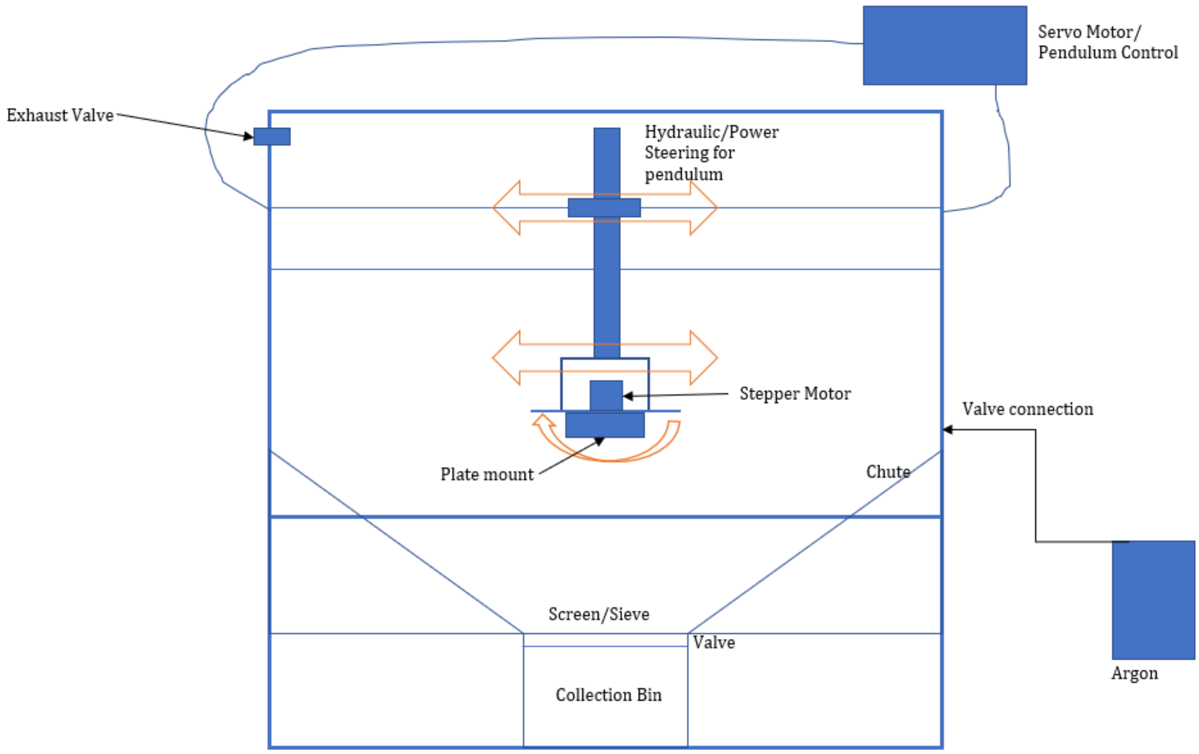

Figure 3:Initial Design 1

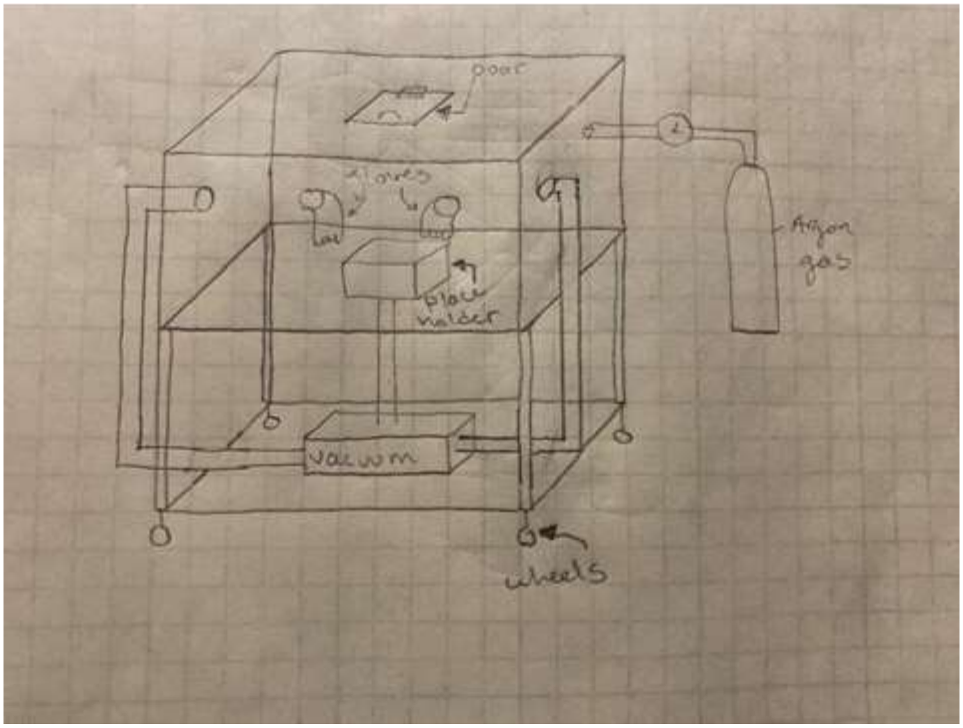

Figure 4: Initial Design 2.

The preliminary mechanical design was a simple pendulum powered by hydraulic steering that would move the additively manufactured part to a 45-degree angle in both directions from the vertical position for a total range of motion of 90 degrees. The part would be mounted on a plate upside down, powered by a motor that would turn and vibrate the part to assist gravity in removing all the powder from small crevices within the part. The powder would then fall into a funneling system through a screen and into a removable compartment to dispose of the powder. The fluid design was made up of a glove box that relied heavily on human interaction with the part. Argon would be blown through tubing to displace the powder in the part while vacuums would be used to draw the powder out. The part would be moved around by hand using the gloves for the vacuum to hit every inch. The designs were compared using the constraints listed in Table 2 and it was decided that the mechanical design fulfilled more functional and design requirements and could be updated to act as a glove box to allow users to inspect parts after they have been cleared of powder.

Table 2. Comparing Mechanical and Fluid Designs

Constraints	Mechanical Design	Fluid Design
Sealed Work Space	Y	Y
Pressurized (1 atm)	Y	N
Computer Automated	Y	N
User Access	N	Y

Inert Environment	Y	N
Motors	Y	N
Compressed Inert Gas	N	Y
Filtration	Y	Y
Part Moved During Cleaning	Y	N
Brush Piece	N	Y

There were several iterations of the mechanical design considered before purchasing and assembling could begin. As seen in Fig. 3, the initial design included controlling the pendulum motion using hydraulic steering. However, after careful consideration of the design, cost, and without the knowledge of the mechanical advantage, the design of the pendulum was changed to a four-bar linkage mechanism as seen in Fig. 5. The final design, as seen in Fig. 6, has a doubled four-bar-linkage on the same side and the gearing in place for the turning of the crank and of the base plate at the end of the pendulum.

Figure 5 Four-bar Linkage

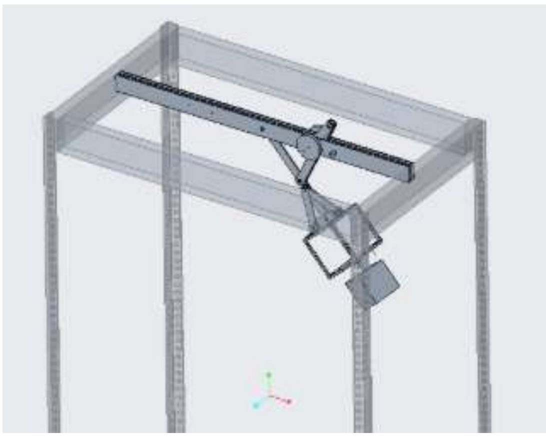

Figure 6 Final Design

3.1.2 Determining Loads and Stresses

The second step of the design process was to determine the loads and stress of key parts of the mechanism to determine if the design is functional and to decide if the materials chosen work. First, initial calculations were done to for the known crucial elements of the design.

One of the essential parts of the device is the four-bar linkage that moves the pendulum. With the initial design, the pendulum was going to use hydraulic steering to function. However, since we did not know the mechanical advantage of the system and the company could not provide it, the switch was made to a four-bar linkage. By doing this, we would know what we needed to adjust the mechanical advantage to buy the appropriate motor. The mechanical advantage of the system is the measure of the ratio of output force to input force, as seen in Equation 1.

$$MA = \frac{Output\ Force}{Input\ Force} = \frac{Input\ Arm\ Distance}{Output\ Arm\ Distance} \qquad MA = \left(\frac{R_{in}}{R_{out}}\right) * \frac{[I_{24}, I_{14}]}{[I_{24}, I_{12}]}$$

Equation 1

In this formula, Rin equals the length of the crank which 3.5 inches. Rout is equal to the length of the pendulum which is 7 inches. $[I_{24}, I_{14}]$ is equal to 10.5 inches and $[I_{24}, I_{12}]$ is equal to 4 inches. From this equation, the mechanical advantage of the system is equal to 1.31.

Another crucial element to the design is the spinning plate. While the pendulum swings, we knew that the base plate of the part would turn as it is moving so that every crevice of the part that may have powder would face the ground and be assisted by gravity throughout the process. In order to decide what type of motor to purchase for the plate, the torque for the spinning of the base needed to be known. The formulas used to determine the torque can be seen in Equation 2.

$$I_L = \frac{1}{2}m(w^2 + h^2) = 0.175041\ lb * ft^2 = 0.0738\ kg * m^2$$

$$T = IA$$

Equation 2

Here A is the angular acceleration which is the change in the angular velocity over the change in time, and I_L is the moment of inertia. Since the need for this mechanism is one rotation per second and one second to accelerate, the angular velocity is simply equal to 2π rad/s and the angular acceleration is equal to 2π rad/s^2 or 6.283 rad/s^2. Plugging I and A back into the initial equation,

$$T = IA = 0.0738\ kg * m^2 \left(6.283 \frac{rad}{s^2}\right) = 0.463\ N * m$$

The other central elements to this design were the pendulum and the support beam for the pendulum. It was important to know the stress the top support beam holding the pendulum, and everything attached to it as well as the forces the pendulum itself would be subject to. The stress for the top support beam was found as shown in Fig. 7.

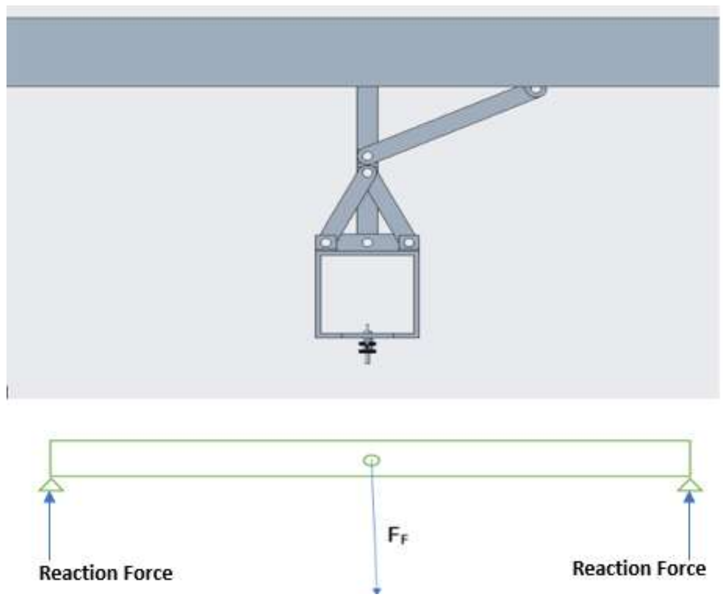

Figure 7 Loads and Stresses on Pendulum Support Beam

$$\sigma_{max} = \frac{y_{max} F L}{4I}$$

$$\sigma_{max} = \frac{(1\ in)(18.07\ lb)(30\ in)}{(4)(0.16667\ in^4)} = 813.134\ psi = 5.61\ MPa$$

As shown, the max stress in the top beam with a load of 18.07 pounds, a length 30 inches, and an inertia of 0.16667 in^4 is equal to 813.134 psi or 5.606 MPa. An analysis was also done on the pendulum link as shown in Fig. 8.

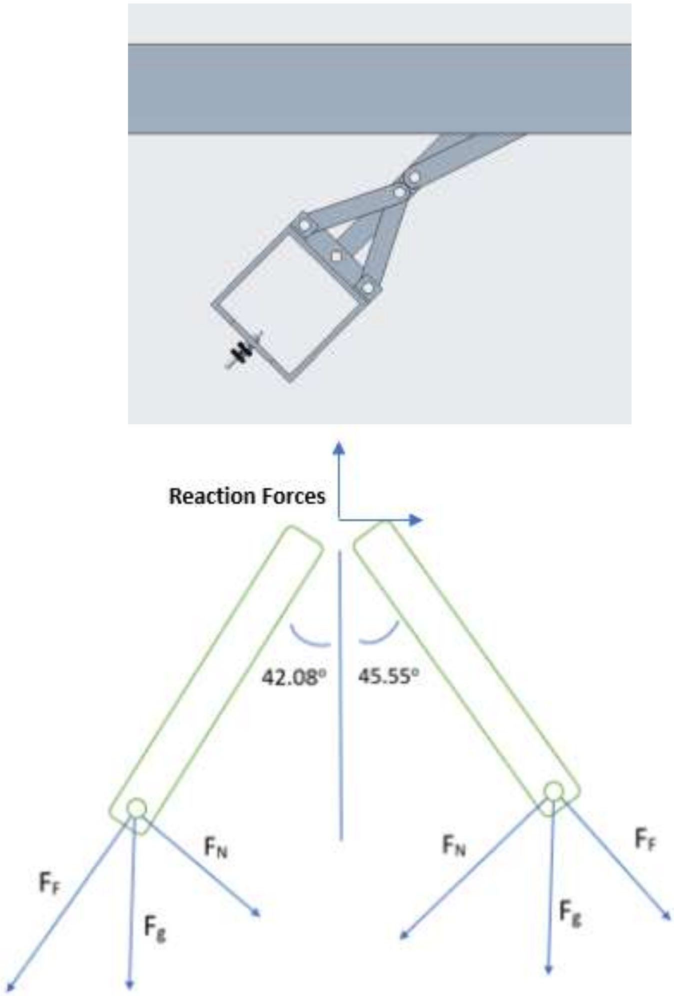

Figure 8 Loads and Stresses on the Pendulum

Load with pendulum vertical:
Preliminary Assumptions: Angular Velocity: 1/3 revolution per second.

$$Angular\ Velocity, \omega = \frac{\frac{2}{3}rad}{s}; Accerleration\ normal, a_n = \omega^2 * r; r = 1.59ft;\ mass = 0.621slugs; gravitaional\ accleration, g = 32.14ft/s^2$$

$$Vertical\ Load, F_y = mass * (g + a_n) = \textbf{22.04 lbs}$$

Load on crank pin, which has to be supported by motor. This maximum load calculation was done with assumption of pendulum at max angle, 45degrees, in a quasi-static situation. The angle of the crank link at this position is 21 degrees. Additional variables include crank link length of 0.583ft.

$$\omega^2 = \omega_0^2 + 2\alpha\theta \Rightarrow \alpha = \frac{\omega^2}{2\theta} = 2.793 rad/s^2$$
$$a = r\alpha = 4.412 ft/s^2$$
$$F_y = m(g + a * sin\theta) = 21.9 lbs$$
$$F_x = m(a * cos\theta) = 1.94 lbs$$
$$F = \sqrt{F_x^2 + F_y^2} = 22 lbs;\ \phi = atan\left(\frac{F_y}{F_x}\right) = 1.48 rad$$
$$\sum M = 0 = F_{link} r_{link} \sin(0.366) - F sin(\phi) r \Rightarrow F_{link} = \frac{rF sin\phi}{r_{link} \sin(0.366)} = 167 lbs$$
$$Two\ Motors, two\ crank\ links, so\ load\ on\ motors\ is\ 83.5 lbs$$

A model of the entire device, Fig. 9 below, was created to determine if the design was feasible. Additionally, this model allowed our team to examine critical components in depth to justify geometric and material decisions. The important features of the device to focus on were the pendulum support beam, crank, crank shaft pendulum link, link pin, motor mount, and the rotating plate shaft.

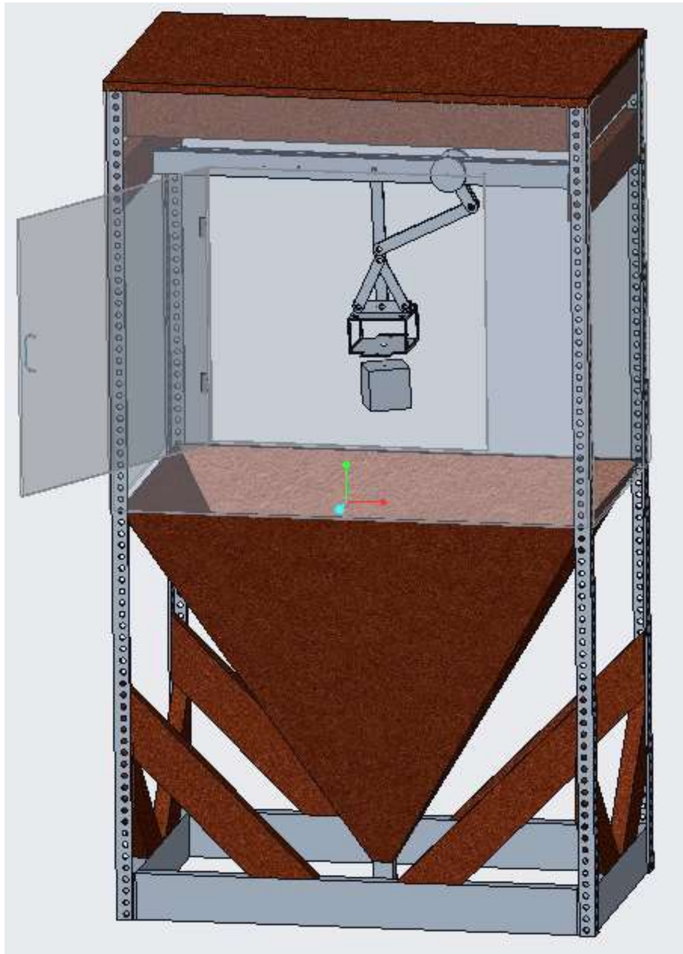

Figure 9 Final Design and Creo Simulation

Initially, position and dynamic analyses were run to gather data from the mechanism to use as parameters in FEA and other calculations. The following graphs were produced by only recording data points that were greater than the last (or less than); this clearly demonstrates the maximum angle position of the pendulum.

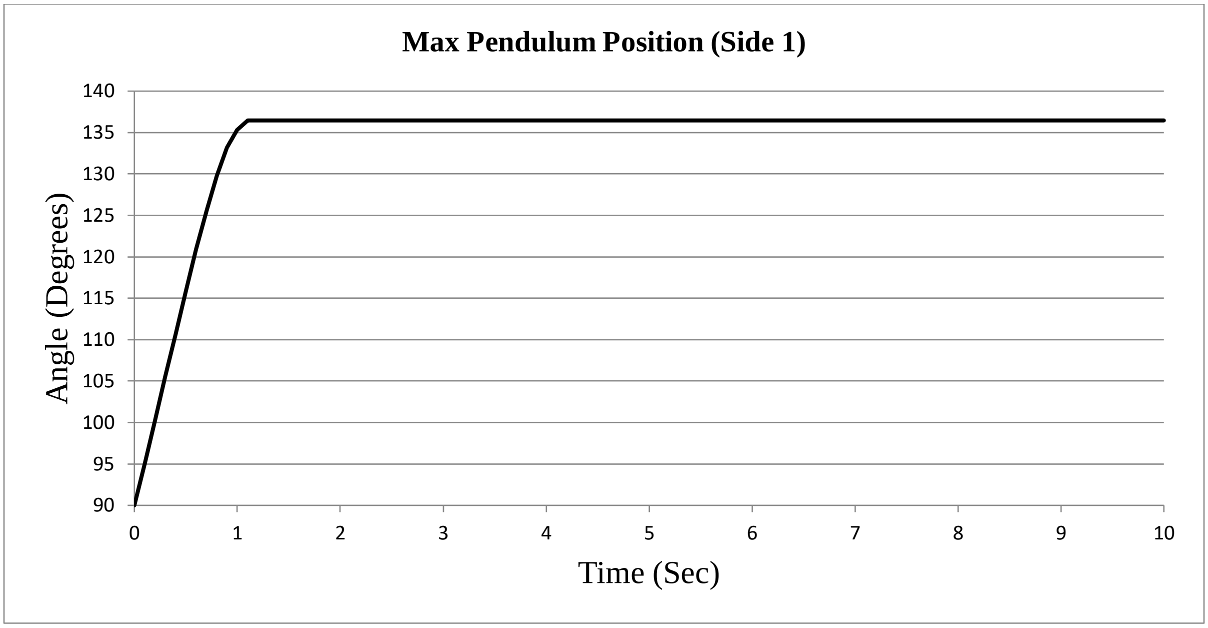

Figure 10 Pendulum Max Angle Side 1

90 degrees represents the straight down position therefore the maximum angle is equal to 136.5-90, which equates to 46.5 degrees.

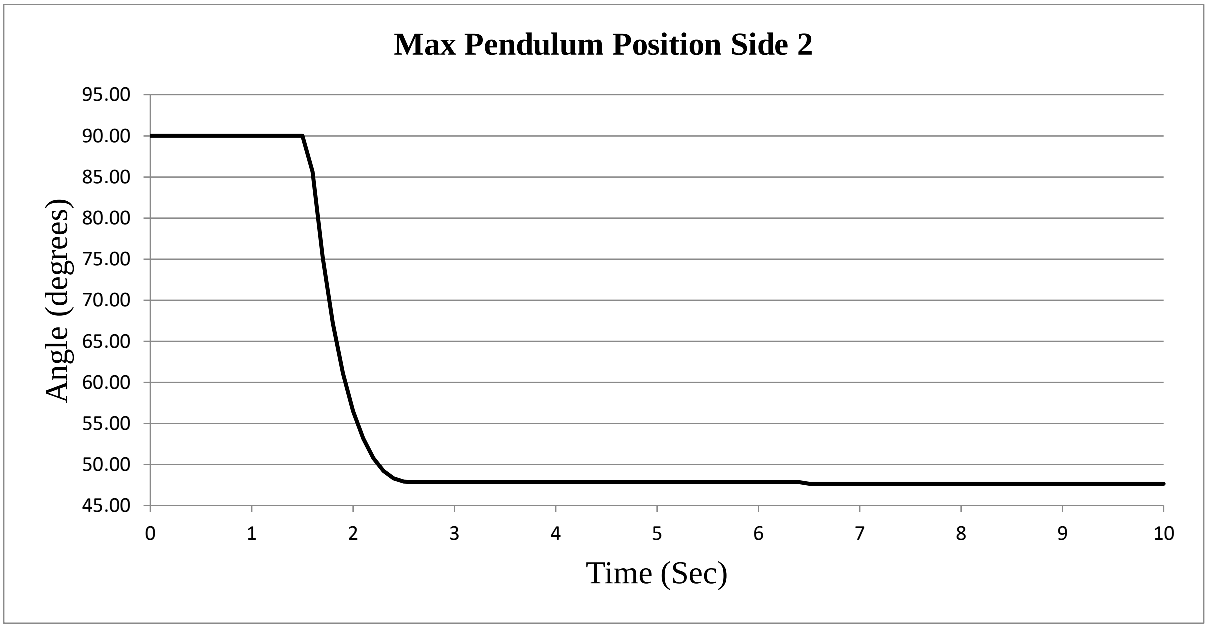

Figure 11 Pendulum Max Angle Side 2

According to this data, the maximum angle on the other side is equal to 90-47.64, which is 42.36 degrees. 46.5≠42.36: This lack of position symmetry of the pendulum forbids the possibility of doubling the 4-bar linkage on the opposing side. All simulations would fail, and prototypes would jam. This is the reason for the linkages being doubled up on the same side.

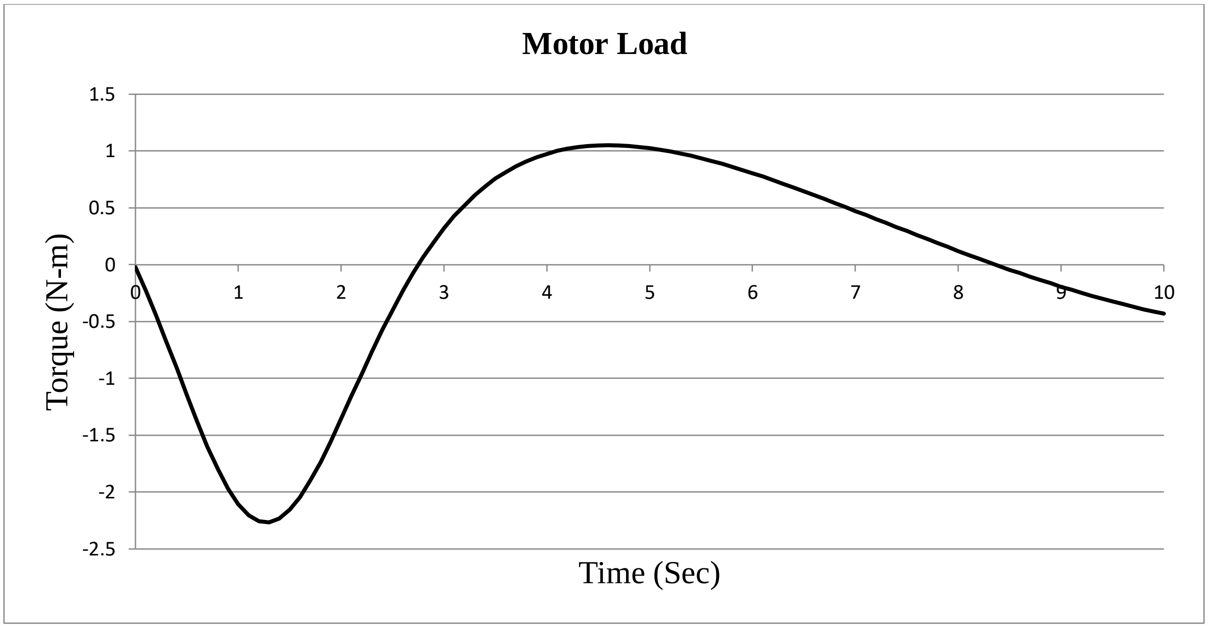

Figure 12 Motor Load

The above graph shows the loading of the motors to power the 4 bar linkages. The maximum torque required is 20 lb-in, or 2.26 N-m. This torque requirement was achieved by using two motors and utilizing gear ratios to increase mechanical advantage.

Crank:

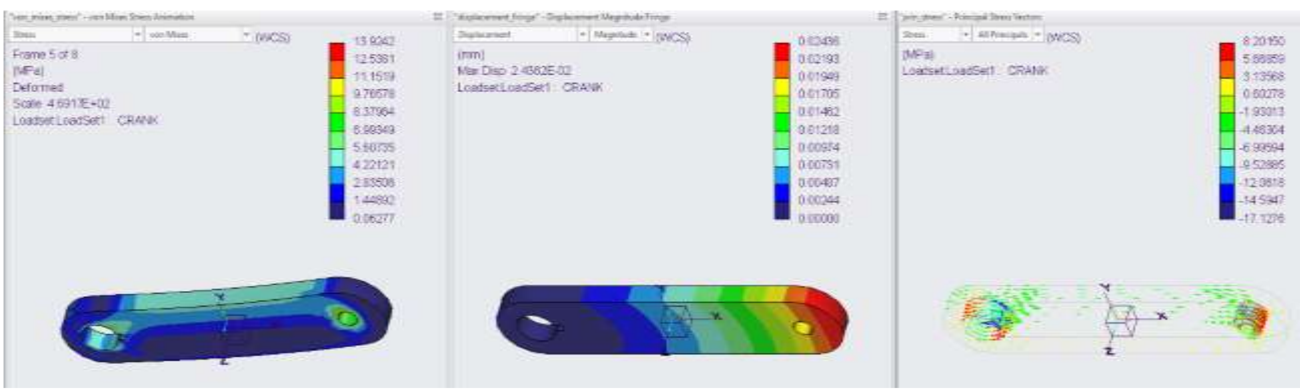

Figure 13 Crank FEA

FEA was done for the crank for its most critical position as seen in Fig. 12. This is when the pendulum is at near max angle, and the crank has the least leverage during the cycle. So, the crank is undergoing a compressive load equal to about the weight of the pendulum plus the part being cleaned. The maximum von mises stress is 13.9 MPa, and the yield strength of aluminum is about 110 MPa: this gives a safety factor of 7.9.

Free Body Diagram:

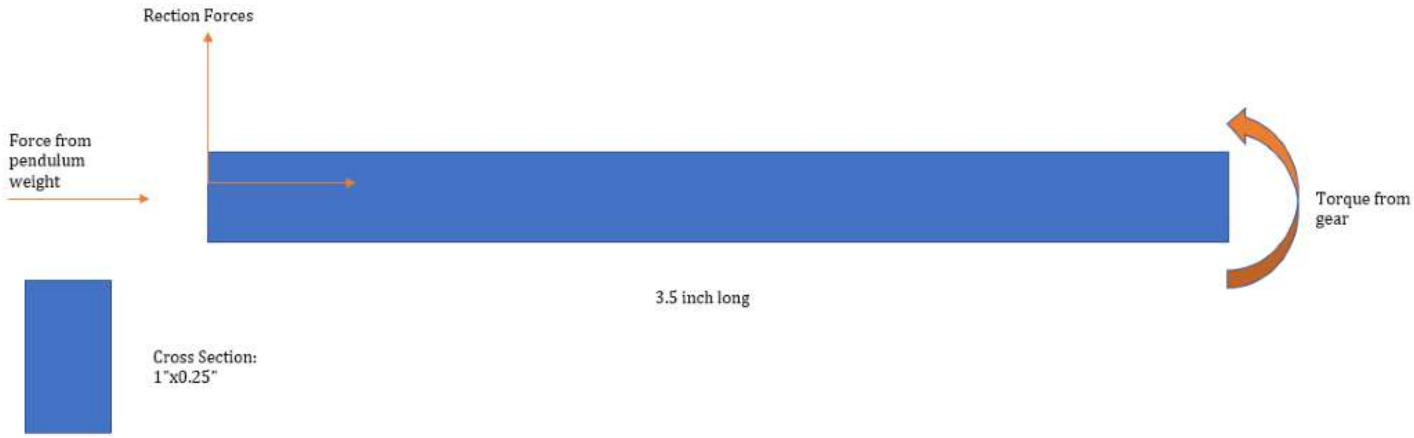

Figure 14 Crank Static Free Body Diagram

Simplified Stress Analysis:

$$b := 0.00635 \qquad M := 2.2 \qquad P := 534$$

$$h := 0.0254$$

$$I := \frac{\left(b \cdot h^3\right)}{12}$$

$$I = 8.671 \cdot 10^{-9}$$

$$\sigma_m := \frac{\left(M \cdot \frac{h}{2}\right)}{I} \qquad \sigma_{comp} := \frac{P}{b \cdot h}$$

$$\sigma_m = 3.222 \cdot 10^6 \qquad \sigma_{comp} = 3.311 \cdot 10^6$$

$$\sigma_{critical} := \sigma_m + \sigma_{comp}$$

$$\sigma_{critical} = 6.533 \cdot 10^6$$

$$\sigma_1 := \sigma_{critical} \qquad \sigma_2 := -\sigma_{critical}$$

$$\sigma_1 = 6.533 \cdot 10^6 \qquad \sigma_2 = -6.533 \cdot 10^6$$

$$\sigma_{vm} := \sqrt{{\sigma_1}^2 - \sigma_1 \cdot \sigma_2 + {\sigma_2}^2}$$

$$\sigma_{vm} = 1.132 \cdot 10^7 \qquad \sigma_{vm}MPa := \frac{\sigma_{vm}}{10^6}$$

$$\sigma_{vm}MPa = 11.315$$

Figure 15 Crank Stress Analysis

The resultant von mises stress is significantly lower than the FEA due to the stress concentration of the relatively small keyway that was ignored in the simplified analysis. The keyway is responsible for majority of the force transfer. Note that critical stress is in where the compression from the bending stress adds with the compressive stress from pendulum load.

Crank Shaft:

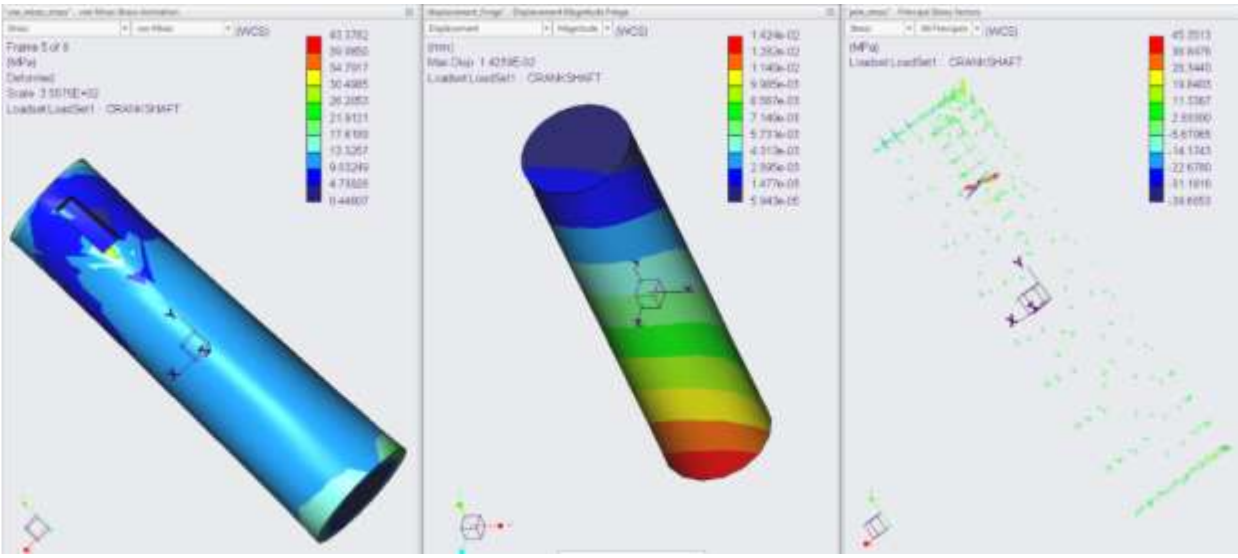

Figure 16 Crank Shaft FEA

The crank shaft was made using steel since diameter was a limited parameter to work with. This gives a safety factor of 8.13.

Free Body Diagram:

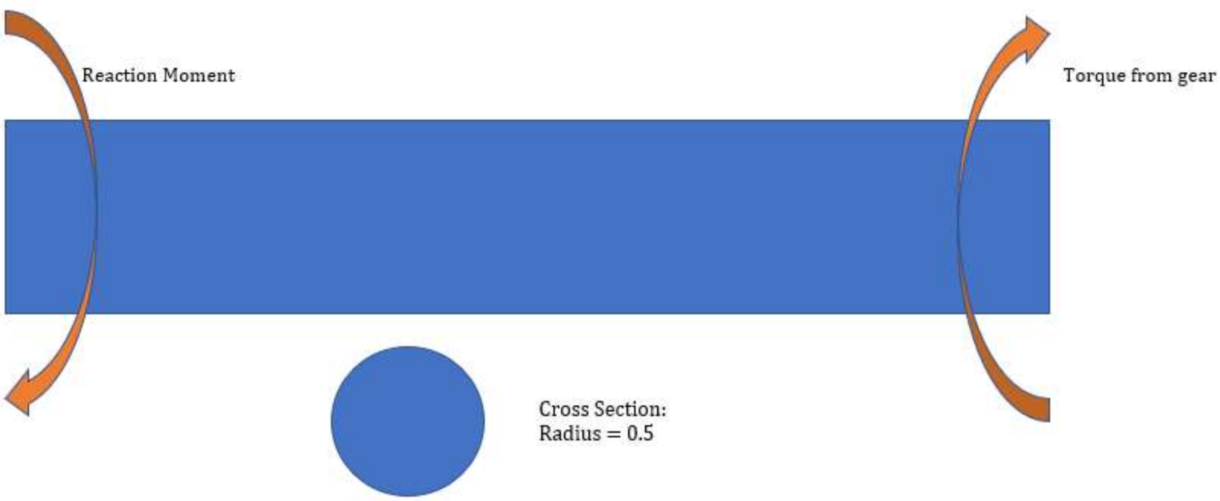

Figure 17 Crank Shaft Static Free Body Diagram

Simplified Analysis:

There is only torsion in this part, so shear stress is the only concern.

$$r := 0.00635 \qquad T := 2.2$$

$$J := \frac{(\pi \cdot r^4)}{2}$$

$$J = 2.554 \cdot 10^{-9}$$

$$\tau := \frac{(T \cdot r)}{J}$$

$$\tau = 5.47 \cdot 10^{6}$$

$$\tau_{MPa} := \frac{\tau}{10^6}$$

$$\tau_{MPa} = 5.47$$

Figure 18 Crank Shaft Stress Analysis

This stress is significantly lower than the simulated result, this is because the torque transfer is completely concentrated at the keyway (similar to the crank link), rather than around the whole cross section, which the simplified analysis assumes.

Pendulum Link:

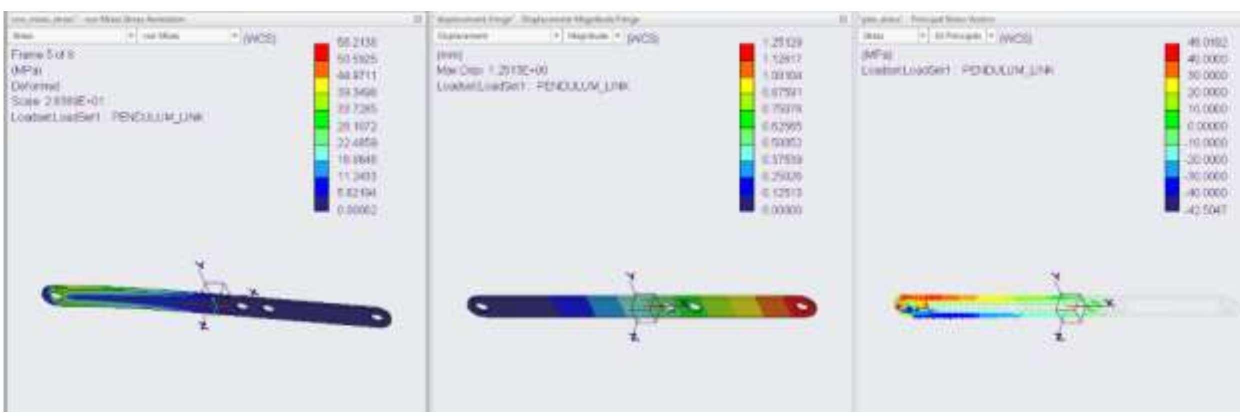

Figure 19 Pendulum Link FEA

FEA was done for the pendulum link as seen in Fig. 19, under its most critical loading, while at its maximum angle. This results in its maximum bending moment, with the crank pulling the center of it up, and the attached part at the bottom pulling down. At its critical loading scenario, the safety factor comes out to 2.2.

Free Body Diagram:

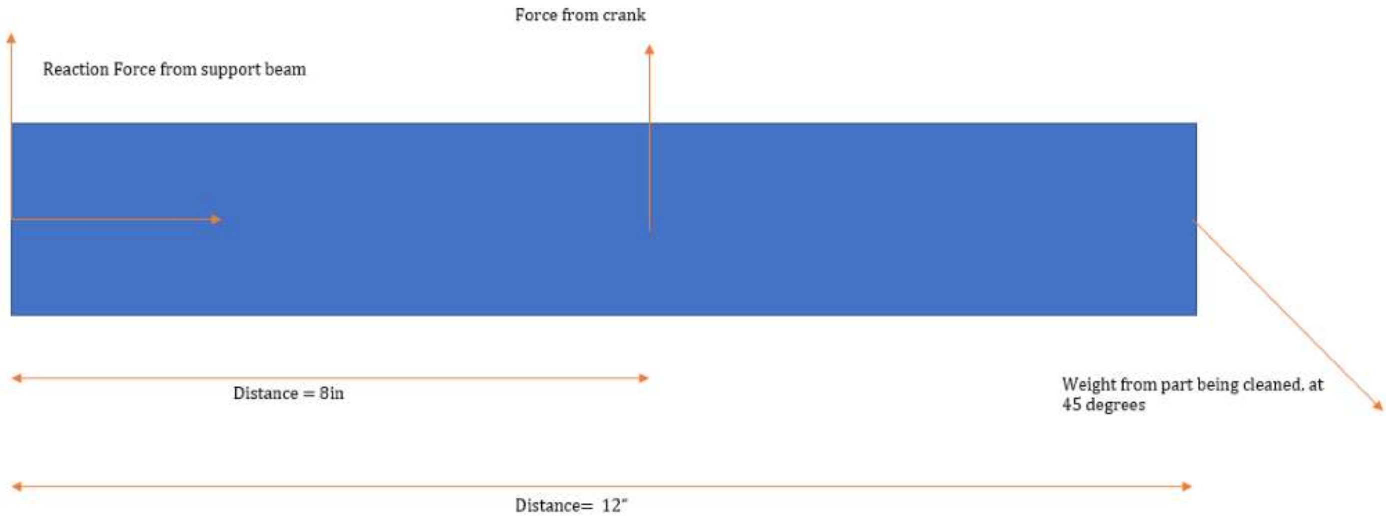

Figure 20 Pendulum Link Static Free Body Diagram

Simplified Analysis:

$R_1 := 49.1 \qquad a := 0.2032 \qquad L := 0.3048$

$S(x,z) := \text{if}(x \geq z, 1, 0)$

$V(x) := R_1 \cdot S(x,0) \cdot (x-0)^0 - 89 \cdot S(x,a) \cdot (x-a)^0 + 78.7 \cdot S(x,L) \cdot (x-L)^0$

$M(x) := R_1 \cdot S(x,0) \cdot (x-0)^1 - 89 \cdot S(x,a) \cdot (x-a)^1 + 78.7 \cdot S(x,L) \cdot (x-L)^1$

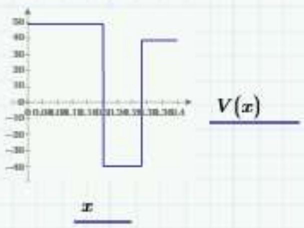

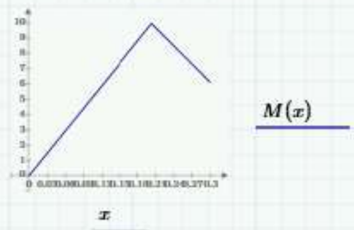

$b := 0.003175 \qquad P := 78.7 \qquad M(a) = 9.977$

$h := 0.0254 \qquad V(a) = -39.9$

$I := \frac{(b \cdot h^3)}{12}$

$I = 4.336 \cdot 10^{-9}$

$\sigma_m := \frac{\left(M(a) \cdot \frac{h}{2}\right)}{I} \qquad \sigma_{ten} := \frac{P}{b \cdot h}$

$\sigma_m = 2.922 \cdot 10^7 \qquad \sigma_{ten} = 9.759 \cdot 10^5$

$\sigma_{critical} := \sigma_m + \sigma_{ten}$

$\sigma_{critical} = 3.02 \cdot 10^7$

$\sigma_1 := \sigma_{critical} \qquad \sigma_2 := -\sigma_{critical}$

$\sigma_1 = 3.02 \cdot 10^7 \qquad \sigma_2 = -3.02 \cdot 10^7$

$\sigma_{vm} := \sqrt{\sigma_1^2 - \sigma_1 \cdot \sigma_2 + \sigma_2^2}$

$\sigma_{vm} = 5.231 \cdot 10^7 \qquad \sigma_{vm}MPa := \frac{\sigma_{vm}}{10^6} \qquad \sigma_{vm}MPa = 52.308$

Figure 21 Pendulum Link Stress Analysis

Due to the more complex loading scenario, singularity loading functions were written as seen in Fig. 21, and then integrated twice to obtain shear and moment functions. This method will also be utilized for other parts when needed. Since the pendulum weight is at angle, that caused a tensile stress along with the expected bending stress. In these calculations, the critical stress point is at the top of the cross section where the tensile stress adds with the tension due to bending. The simplified analysis is slightly off due to the holes in the real model serving as stress concentrations, however significantly more accurate than parts with keyways.

Pendulum Support Beam:

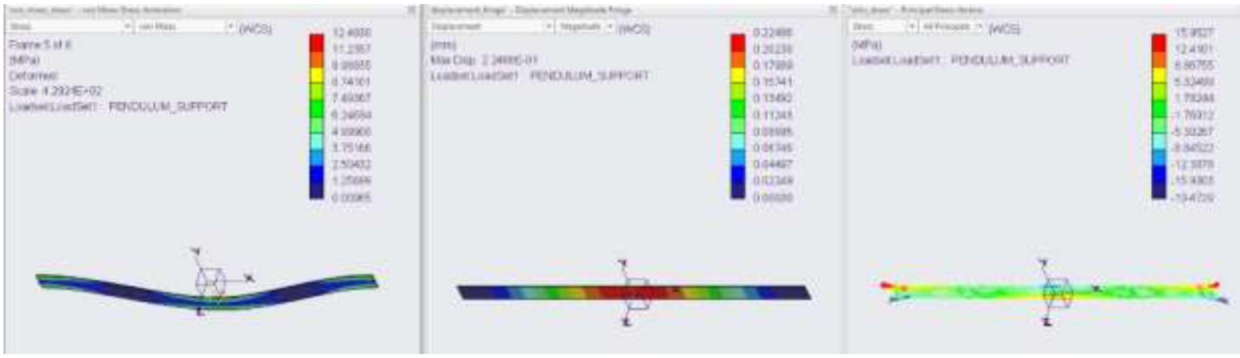

Figure 22 Pendulum Support Beam FEA

This is another critical component as it supports the working mechanism, the stresses within this beam are well under the yielding strength, at 12.5 MPa, resulting in a safety factor of 8.8 as seen in Fig. 22.

Free Body Diagram:

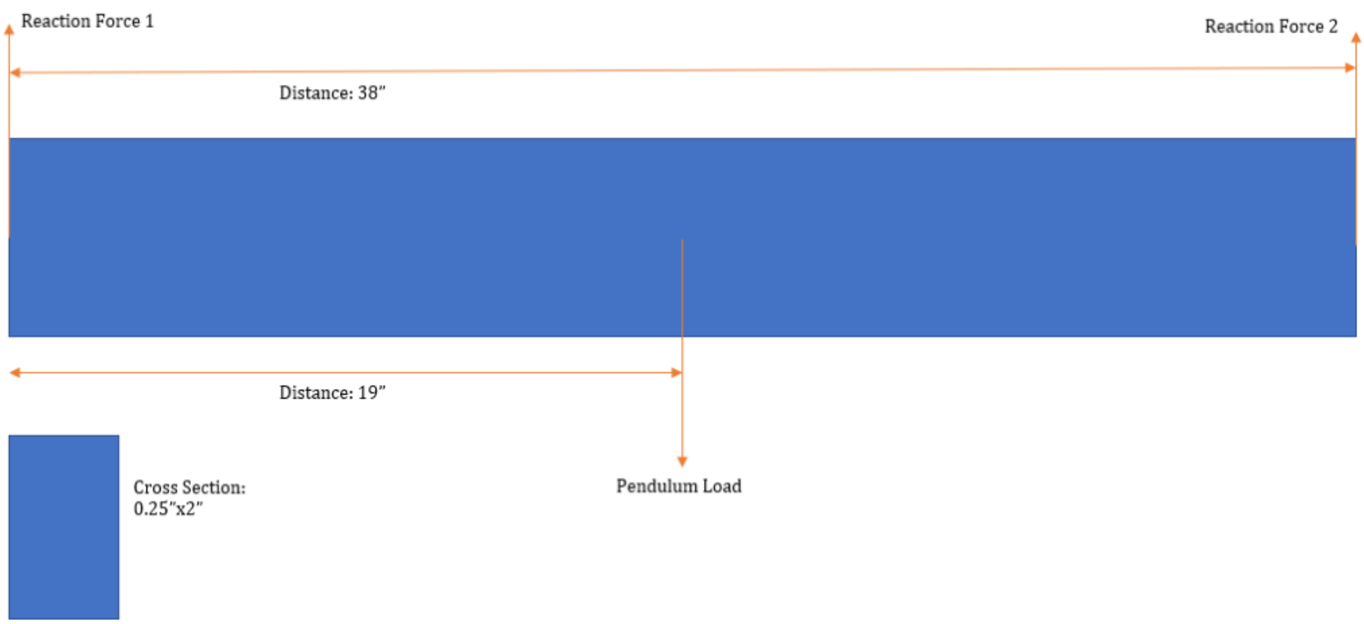

Figure 23 Pendulum Support Beam Static Free Body Diagram

Simplified Analysis:

$R_1 := 45 \qquad R_2 := 45 \qquad a := 0.4826 \qquad L := 0.97$

$S(x,z) := \text{if}(x \geq z, 1, 0)$

$V(x) := R_1 \cdot S(x,0) \cdot (x-0)^0 - 90 \cdot S(x,a) \cdot (x-a)^0 + R_2 \cdot S(x,L) \cdot (x-L)^0$

$M(x) := R_1 \cdot S(x,0) \cdot (x-0)^1 - 90 \cdot S(x,a) \cdot (x-a)^1 + R_2 \cdot S(x,L) \cdot (x-L)^1$

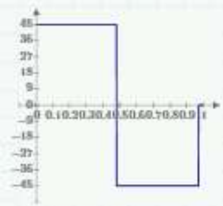

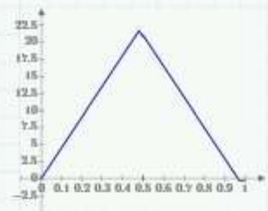

$b := 0.00635$

$h := 0.0508$

$M(a) = 21.717$

$V(a) = -45$

$I := \frac{(b \cdot h^3)}{12}$

$I = 6.937 \cdot 10^{-8}$

$\sigma_m := \frac{\left(M(a) \cdot \frac{h}{2}\right)}{I}$

$\sigma_m = 7.952 \cdot 10^6$

$\sigma_1 := \sigma_m \qquad \sigma_2 := -\sigma_m$

$\sigma_1 = 7.952 \cdot 10^6 \qquad \sigma_2 = -7.952 \cdot 10^6$

$\sigma_{vm} := \sqrt{\sigma_1^2 - \sigma_1 \cdot \sigma_2 + \sigma_2^2}$

$\sigma_{vm} = 1.377 \cdot 10^7 \qquad \sigma_{vm}MPa := \frac{\sigma_{vm}}{10^6} \qquad \sigma_{vm}MPa = 13.772$

Figure 24 Pendulum Support Beam Stress Analysis

This analysis seen in Fig. 24 resulted in a slightly higher von mises stress than the FEA, however this still a very accurate analysis despite that is simplified.

Build Plate Shaft:

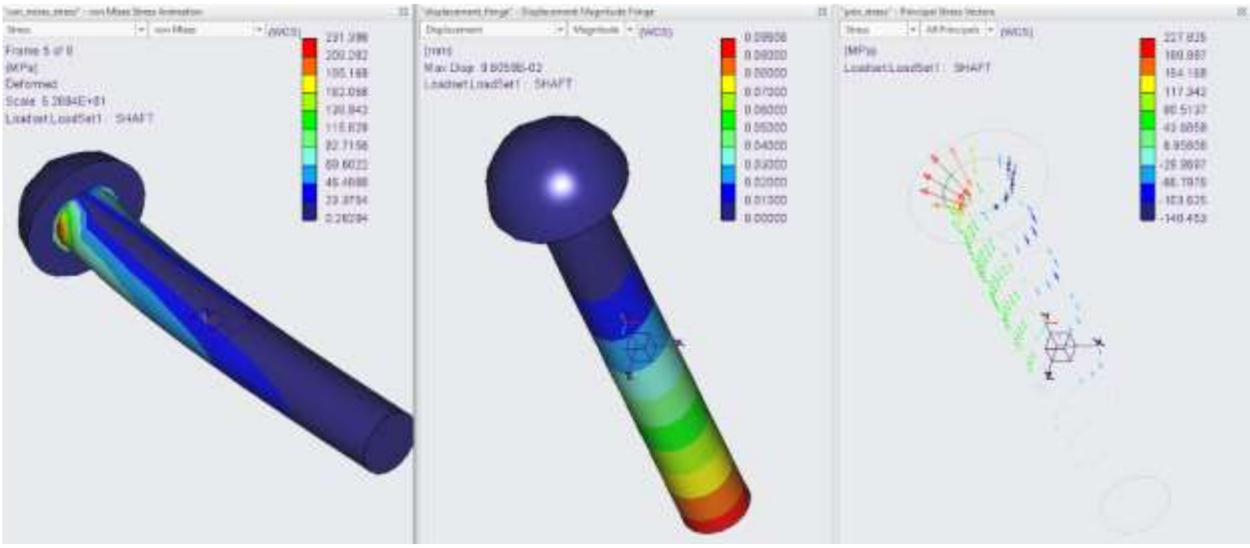

Figure 25 Build Plate Shaft FEA

This component depicted in Fig. 25 is responsible for supporting the rotating plate and attached part for cleaning. This relatively small component supports a large load and therefore undergoes large stresses; it needs to be a steel part, as aluminum would yield and deform too easily. The yield strength of steel is 350 MPa. So, the safety factor is 1.2

Free Body Diagram:

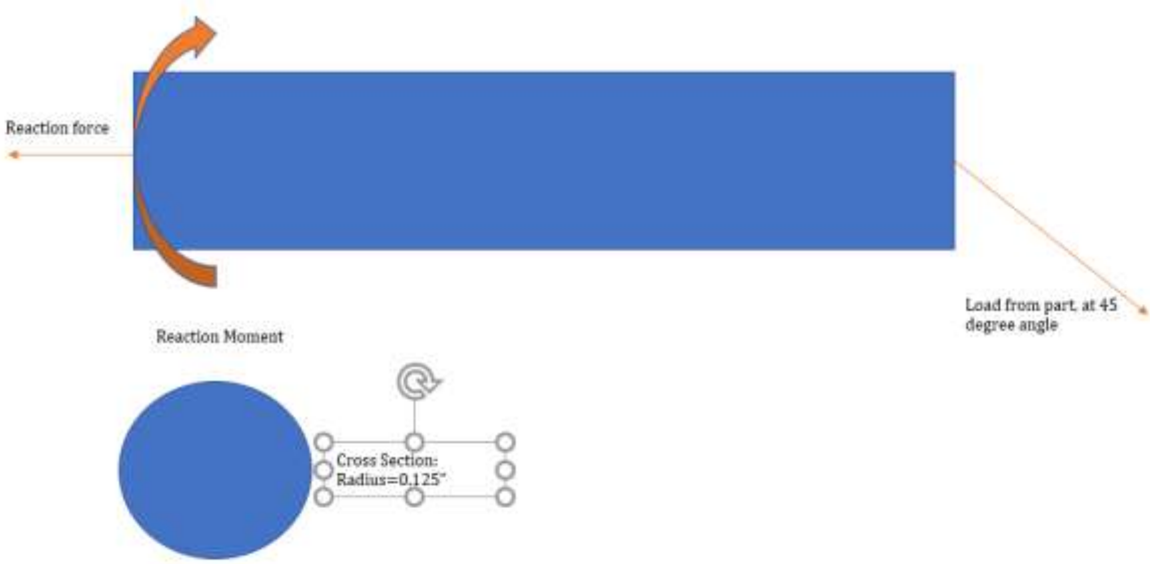

Figure 26 Build Plate Shaft Static Free Body Diagram

Simplified Analysis:

$R_1 := 3.39 \qquad L := 0.0508$

$S(x,z) := \mathrm{if}(x \geq z, 1, 0)$

$M(x) := R_1 \cdot S(x,0) \cdot (x-0)^0 + 66.7 \cdot S(x,L) \cdot (x-L)^1$

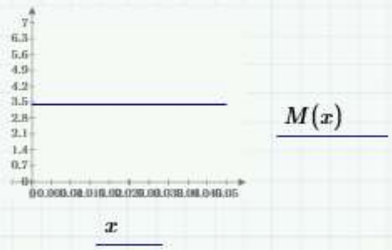

$M(0) = 3.39 \qquad r := 0.00635 \qquad P := 66.7$

$I := \frac{(\pi \cdot r^4)}{4} \qquad A := \pi \cdot r^2$

$\sigma_m := \frac{(M(0) \cdot r)}{I} \qquad \sigma_{ten} := \frac{P}{A}$

$\sigma_m = 1.686 \cdot 10^7 \qquad \sigma_{ten} = 5.265 \cdot 10^5$

$\sigma_{critical} := \sigma_m + \sigma_{ten}$

$\sigma_{critical} = 1.738 \cdot 10^7$

$\sigma_1 := \sigma_{critical} \qquad \sigma_2 := -\sigma_{critical}$

$\sigma_1 = 1.738 \cdot 10^7 \qquad \sigma_2 = -1.738 \cdot 10^7$

$\sigma_{vm} := \sqrt{\sigma_1^2 - \sigma_1 \cdot \sigma_2 + \sigma_2^2}$

$\sigma_{vm} = 3.011 \cdot 10^7 \qquad \sigma_{vm}MPa := \frac{\sigma_{vm}}{10^6}$

$\sigma_{vm}MPa = 30.11$

Figure 27 Build Plate Shaft Stress Analysis

This analysis is way too far off to be considered accurate. This is because the actual model has a head (with larger diameter), that take supports the entire reaction moment. The edge is a corner, so in terms of stress concentration charts, the radius/diameter ratio approaches zero, which drives up the stress concentration factor significantly, depicted below. Referring to the FEA diagram of von mises stress, it is clear that almost all the stress is along the edge of the shaft and the head.

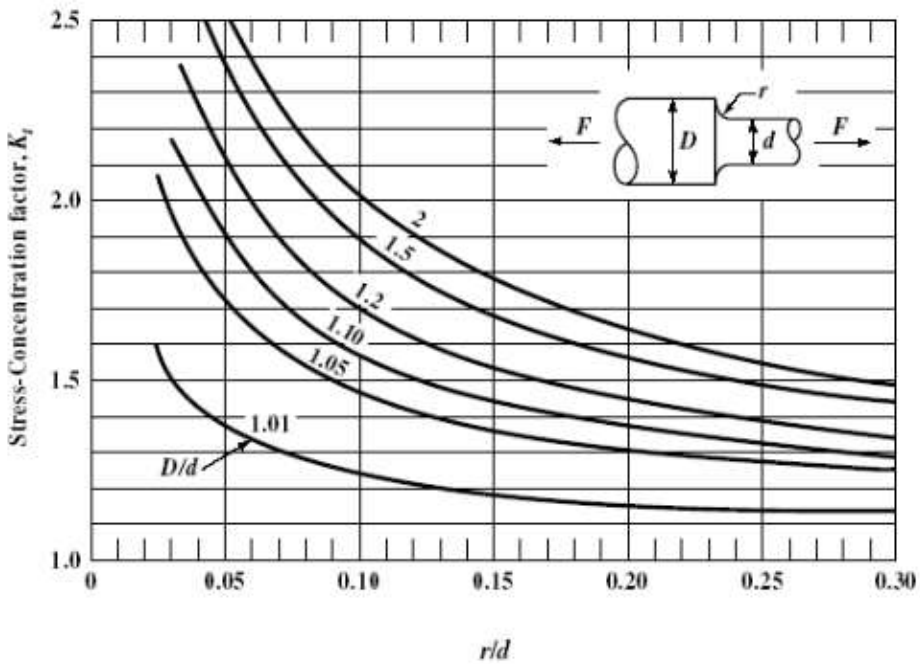

Figure 28 Stress Concentration Chart

Motor Mount:

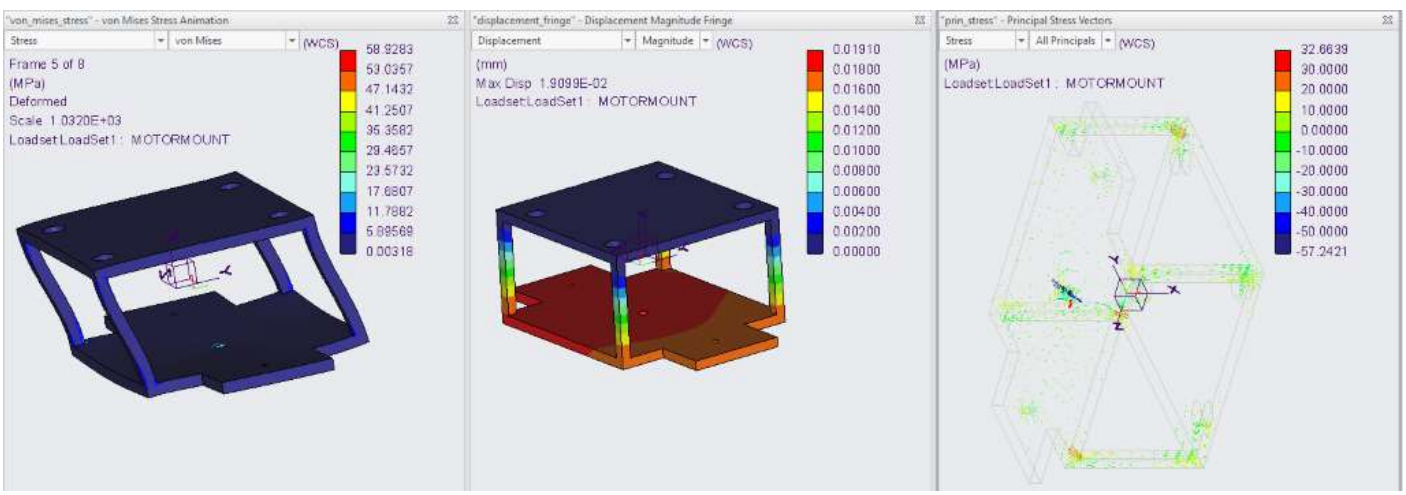

Figure 29 Motor Mount FEA

The motor mount as seen in Fig. 29 is responsible for supporting the build plate, and the gear-belt mechanism that rotates the plate. This is another part that will be steel as to limit deformation as much as possible to ensure the mechanism runs smoothly. This part has a safety factor of 5.8. A simplified analysis for this part is not done as it is complex three-dimensional stress scenario, and accuracy is unlikely. Relying on the finite element analysis is more viable.

Link Pin:

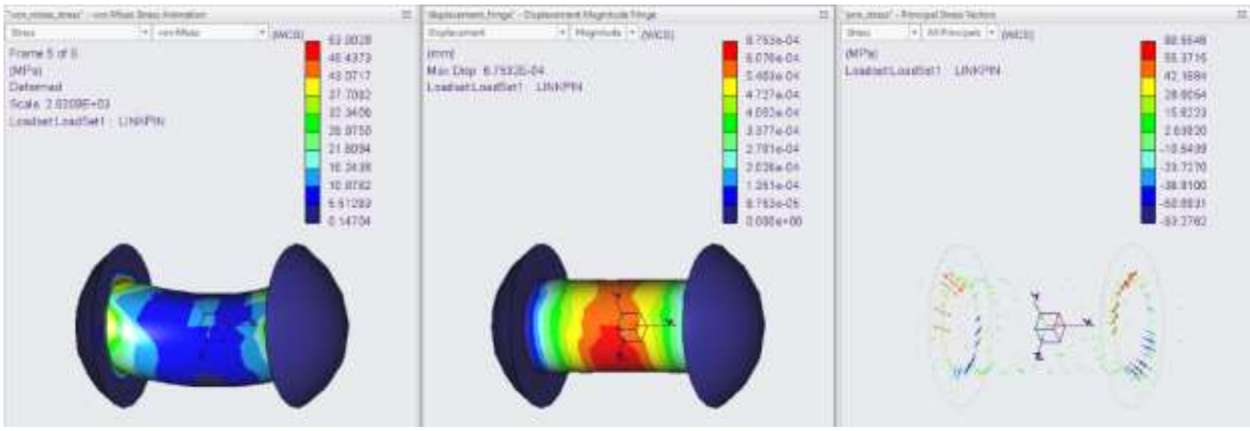

Figure 30 Link Pin FEA

This pin seen in Fig. 30 for the four-bar mechanism is crucial, as it transfers significant loads from link to link. Steel should be used for this part, as the linkage performance depends on sturdy, reliable connections. A safety factor of 5.8 is achieved with this pin design.

Simplified Analysis:

$$R_1 := 3.39 \qquad L := 0.0508$$

$$M := 5.3 \qquad r := 0.00635$$

$$I := \frac{(\pi \cdot r^4)}{4}$$

$$\sigma_m := \frac{(M \cdot r)}{I}$$

$$\sigma_m = 2.636 \cdot 10^7$$

$$\sigma_1 := \sigma_m \qquad \sigma_2 := -\sigma_m$$

$$\sigma_1 = 2.636 \cdot 10^7 \qquad \sigma_2 = -2.636 \cdot 10^7$$

$$\sigma_{vm} := \sqrt{\sigma_1{}^2 - \sigma_1 \cdot \sigma_2 + \sigma_2{}^2}$$

$$\sigma_{vm} = 4.565 \cdot 10^7 \qquad \sigma_{vm}MPa := \frac{\sigma_{vm}}{10^6}$$

$$\sigma_{vm}MPa = 45.648$$

Figure 31 Link Pin Stress Analysis

This is close to the FEA, but slightly off due to unaccounted stress concentrations.

3.1.3 Final Design

The building process took the final design and brought it to fruition. Based on the calculations and tests from the design process, a full material list was developed for every piece needed for the device. The process also included the assembly procedure which incorporated the construction of the framing, all the links, the caging, as well as the setup of the motors with the power supplies and Arduino.

3.1.4 Materials Selection

Bill of Materials

- (2x) Nema 17 2A 59Ncm motors
- (2x) Nema 17 4A 9-42 V Stepper Motor Driver CNC Controller
- (2x) Nema 17 mounting bracket
- (2x) Nema 23 3Nm CNC Stepper Motor
- (2x) CNC Stepper Motor Driver 1-4.2A 20-50VDC for Nema 23
- (2x) Nema 23 mounting bracket
- (2x) 10amp 24 V AC->DC power supplies
- 18-gauge wire (50ft)
- (2x) Power cables
- Breadboard
- Breadboard wires (package of 120)
- Arduino Mega
- 4x 4'x8' MDF Panel Board
- ¾" bolts and nuts
- Tin 3"x3" container
- Kwik Seal adhesive plus Caulk
- 4'x8' plywood
- 1'x1' acrylic glass window
- 2x 1" door hinges
- 1" door handle
- ½" x 17' Gasket weather strip
- 2" zinc plated window bolt
- 3 ½" Zinc-plated Latch Post Safety Hasp
- 2x 2"x4"x42" wood
- 2x 2"x4"x36" wood
- 1 ½" screws

3.2 Building Process

We have the base, links, cage, and side windows built. We used wood for the main base and Zinc L brackets for the side and bolted them together as seen in Fig. 32.

Figure 32 Main Base

We then proceeded to add two of the sides using acrylic pieces to the upper half of the design as seen in Fig. 33. This was then bolted to the Zinc L frame and a wooden top piece was added for structural support.

Figure 33 Frame

Acrylic was used to make windows on the two smaller sides, and they were bolted to the zinc frames. This was to make sure that it was as close to the zinc, and then we used liquid nail to make a complete sealant.

During the design process, we realized that using steel would be difficult to mold into the specified links. Instead, we used Aluminum and cut it down to ¼" due to its pricing and that it is easier to machine than ½". With these pieces we used a simple grinder and ground them down. Then proceeded with a ¼" bit to drill the holes into the links seen in Fig. 34 below.

Figure 34 Pendulum Link

Figure 35 Motor Mount

We then made main bottom frame out of two steel plates and four threaded rods that we bolted together as seen in Fig. 35. We made the steel plates four inches apart so that there is enough space for the two motors that go inside. The main frame was bolted to an aluminum cross sectional beam with two other aluminum links for support. The aluminum links were then together with the sleeve screws as joints because they have no friction.

We then added the bottom two motors by bolting the motor mounts down to the bottom steel plate. We drilled a ¾" hole in the middle of the plate were the middle rod runs through. This rod contains the two gears that the two motors spin. This rod will then be connected to the main steel plate that molds the design block as seen in Fig. 36.

Figure 36 Motor Mount with the Motors

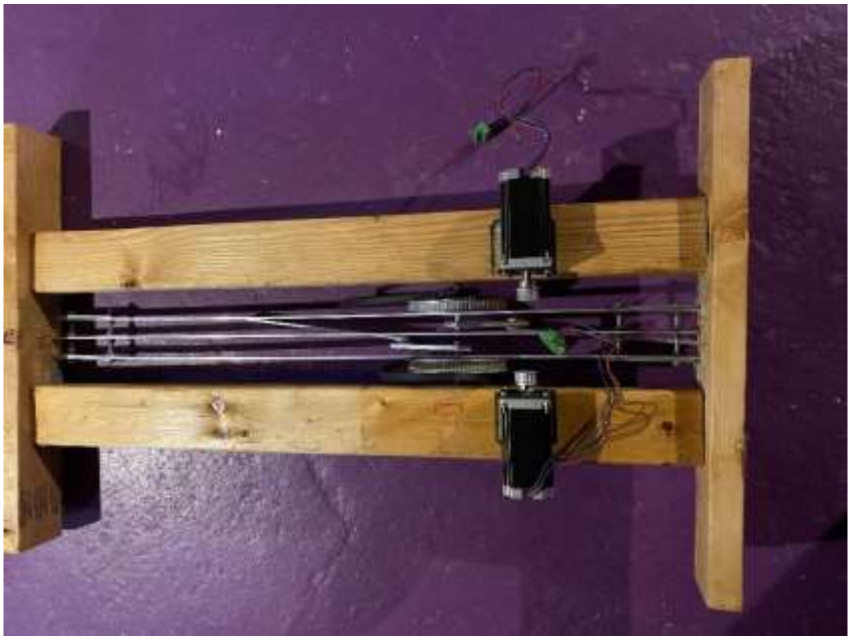

Figure 37 Top Support Beams

We built a motor mount that sits 4" below the top of the main frame as seen in Fig. 37. This is made out of two 2"x4" pieces of wood as the mount for the motors, two 2"x4" pieces of wood as the side railings to mount it on the main frame, three 32" aluminum links that are separated ½" apart, bolts and nuts to keep the aluminum links secured, and metal elbow joints to bolt the aluminum to the wooden frame. We measured the length of the rubber belt to the placement of the motors and drilled small pilot holes into the wooden rails to bolt down the metal motor mounts. This was to ensure that the belt as enough tension to support the load of the pendulum and not slip of the gears during motion. Because there are two gears, there must be two gear rods at each gear for each one to individually rest on. These rods were milled to be able to hold a key fitting to allow the gears and the links to not slip during the rotation of the motors. Finally, we cut a small groove into the underside of the motor mounts to apply a ball bearing mount to support the rods that the gears rest on.

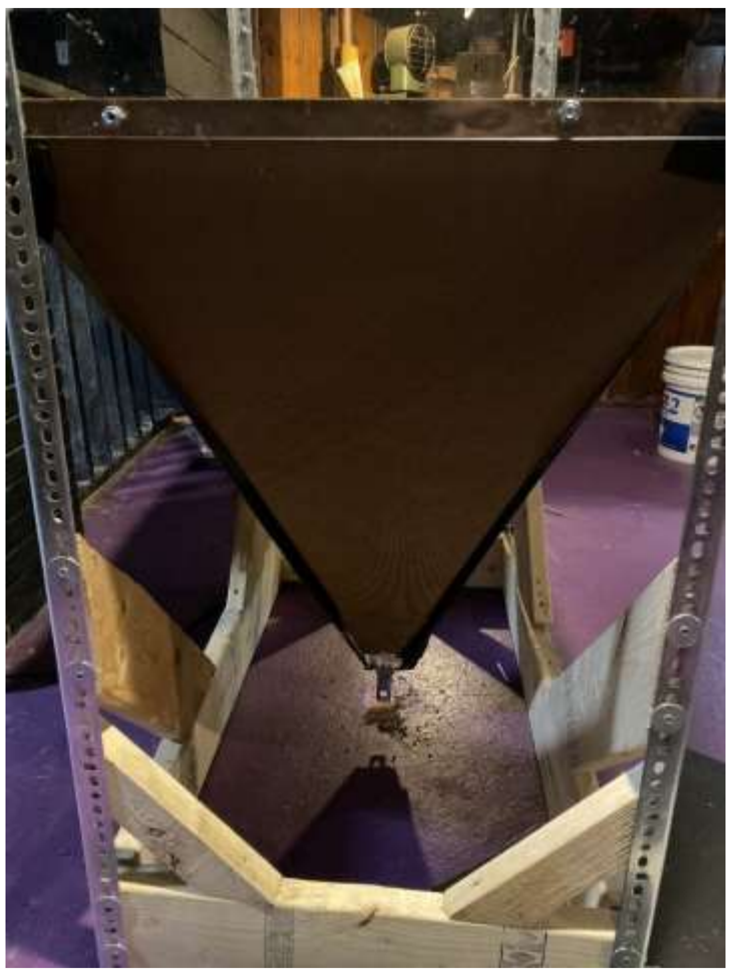

Figure 38 Chute System

We used four pieces of MDF panel board that we cut into two different trapezoids. We made them as large as possible to give the funnel system a steep decline to make all the left-over powder. We then used Gorilla Tape and taped the trapezoid pieces together as a temporary mount. We then used liquid nail and caulked the inside connections of the chute system to make a complete seal as seen in Fig. 38. We then bolted this system to the inside of the main frame and caulked the connection to create a complete seal. The bottom part of the chute has a metal tin container that attaches to the chute with a metal latch. This latch compresses the tin container against a door gasket lining to create a sealant.

One of the more complex and challenging pieces of this project to manufacture was the power transmission link and shaft from the motors to the pendulum. Our team initially tried to use a press fit technique in which the hole of the crank is undersized a few thousands of an inch then the shaft is pressed through to make a tight bond. Our team attempted this twice but the aluminum we were using was too soft for this technique. Our team then brainstormed with manufacturing experts in Washburn in addition to our advisors to attempt a key and slot method of power transmission. This would require extremely precise techniques, mainly the use of wire electrical discharge machining or EDM. Wire EDM machining (Electrical Discharge Machining) is an electro thermal production process where a thin single strand metal wire, along with de-ionized water (used to conduct electricity) allows the wire to cut through metal by the use of heat from electrical sparks, while preventing rust. The results of this worked extremely well as seen in Figures 39-41 below.

Figure 39 Crank Arms With Keyway A

Figure 40 Crank Arms with Keyway B

Figure 41 Full Mechanism Attached

We used the same particle board material as the chute system as the other walls. One of the walls has a 2’x2’ acrylic door that has a door gasket as a lining to create a sealant. It then uses a metal latch to close the door. The top wall has all the electrical systems on top and the wires are fed through a small hole that is caulked for a sealant as seen in Fig. 42 and Fig. 43 below. All the walls are then caulked on the inside to create a full sealant inside.

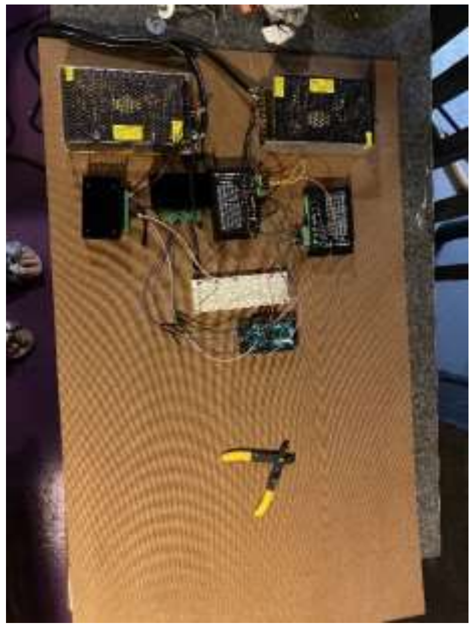

Figure 42 Walls with Electrical System Attached A

Figure 43 Walls with Electrical System Attached B

The second part of the assembly procedure consisted of setting up power supplies, the motors and drivers, and the Arduino to control them. The power supply was prepped by cutting off the female end of the power cable, splicing and striping around a centimeter of wire. The wire was then attached to its respective inlet (Live, Neutral, and Earth). These wires were then screwed down and the cover was closed. The power supply was then plugged in and voltage was measured using a multimeter. We noticed that they were reading .5 volts high, so we used the included potentiometer to correct this. We then repeated the splicing and stripping process for the 18-gauge wire to attach to two positive and two negative terminals on the supplies to power the stepper motor drivers.

The stepper motors and drivers were assembled by first correctly setting the flip switches on the drivers to the desired steps per rotation and current required. Breadboard wires and power cables (the 18-gauge mentioned above) were then attached to each respective terminal and wired according to the schematic below.

The Arduino was plugged in using either a computer USB port when programing or a 9V power supply when in operation. The code above written above was then uploaded and altered to achieve the desired speed of the motors.

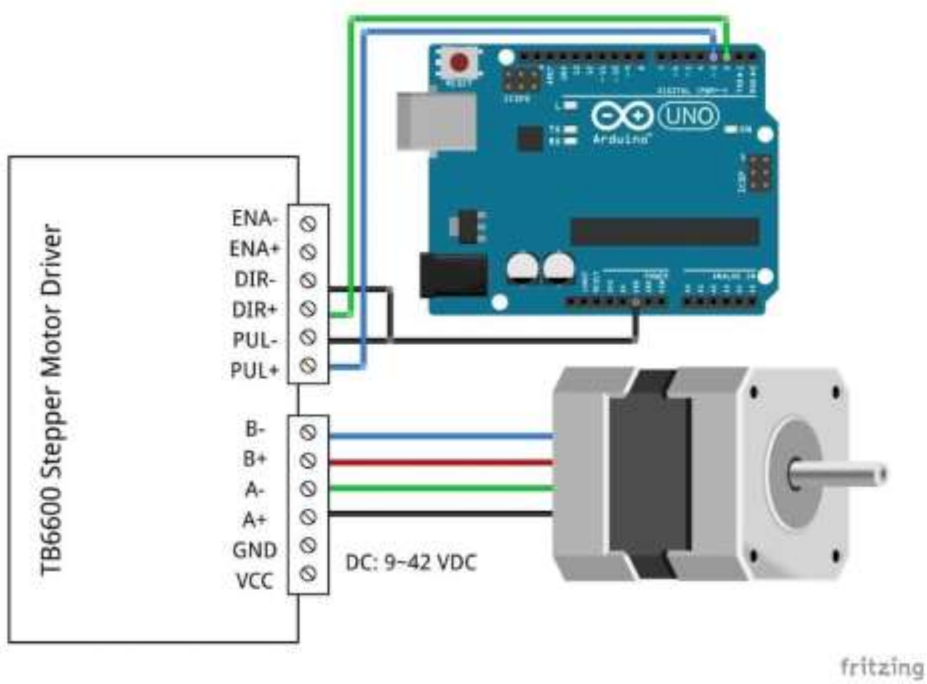

Figure 44 Arduino – Motor Configuration

General guideline for wiring seen in Fig. 45 and Fig. 46, created a common ground using a breadboard and each subsequent motor is attached to two additional Arduino digital outputs.

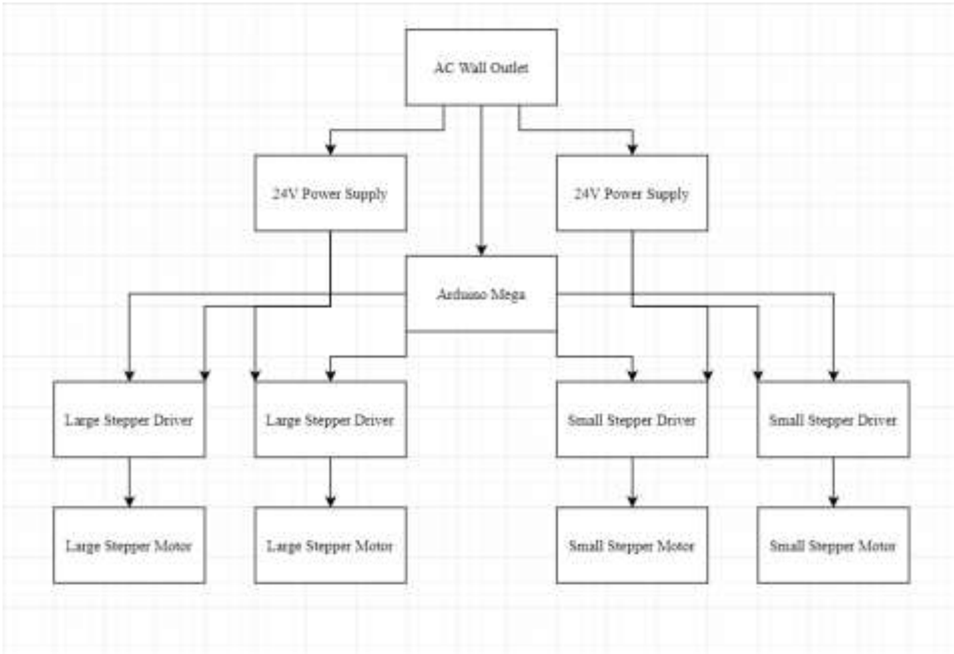

Figure 45 Wiring Guideline

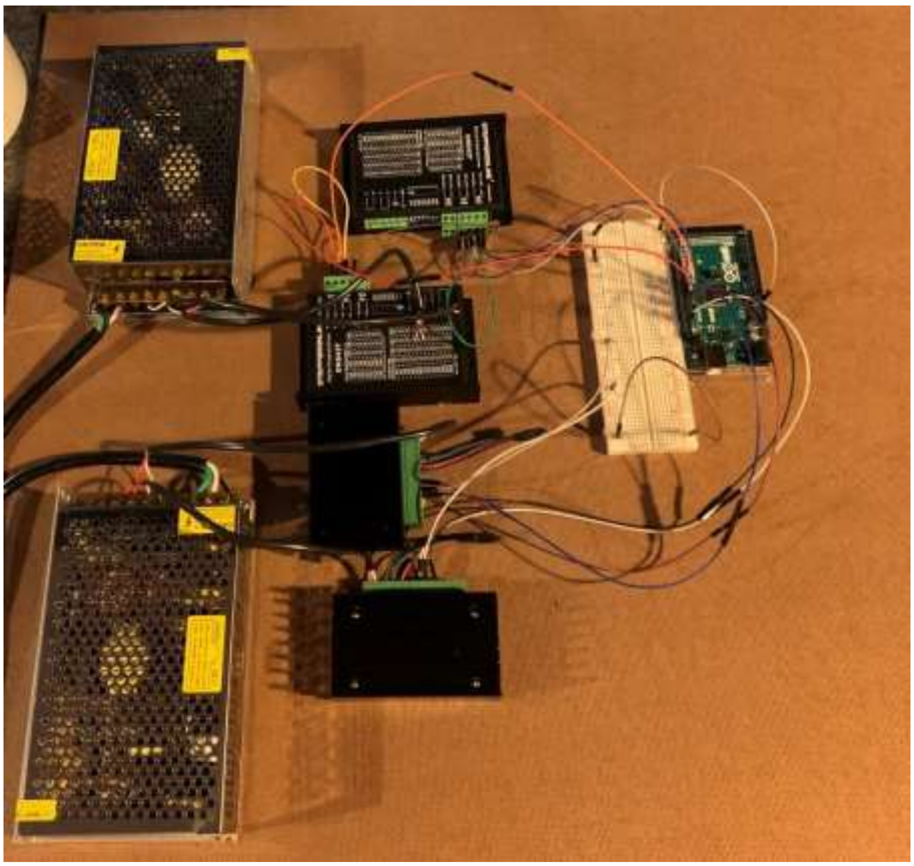

Figure 46 Final Wiring Setup

The final portion of assembly was creating a simple Arduino code seen in Fig. 47 that ran all four motors at once and had the ability to adjust the speeds of these motors. Attached below is the code that this team used for this apparatus to work. The benefit of using an Arduino and stepper motors is this allows for the creation of part specific programs in order to further the accuracy and efficiency of this apparatus.

ConstantSpeed_MQP_Working | Arduino 1.8.10

File Edit Sketch Tools Help

ConstantSpeed_MQP_Working

```
#include <AccelStepper.h>

AccelStepper stepper1(AccelStepper::FULL2WIRE, 2, 3);
AccelStepper stepper2(AccelStepper::FULL2WIRE, 4, 5);
AccelStepper stepper4(AccelStepper::FULL2WIRE, 8, 9);
AccelStepper stepper5(AccelStepper::FULL2WIRE, 10, 11);

void setup()
{
   stepper1.setMaxSpeed(1000);
   stepper1.setSpeed(300);

   stepper2.setMaxSpeed(1000);
   stepper2.setSpeed(300);

   stepper4.setMaxSpeed(1000);
   stepper4.setSpeed(300);

   stepper5.setMaxSpeed(1000);
   stepper5.setSpeed(300);
}

void loop()
{
   stepper1.runSpeed();
   stepper2.runSpeed();
   stepper4.runSpeed();
   stepper5.runSpeed();
}
```

Figure 47 Arduino Code for Running the Motors

4. Results

4.1 Build Summary

This project team was able to conceptualize, design, analyze and build a functional apparatus with the goal of removing residual powder from additively manufactured parts. We were able to employ skills that included computer aided design, structural simulation software, wood and metal craftsmanship, computer coding, computer aided machining, wire electrical discharge machining, and circuit wiring. Due to unforeseen circumstances, this project team was unable to perform a final test on our apparatus but, we were able to confirm the function of all major systems working together.

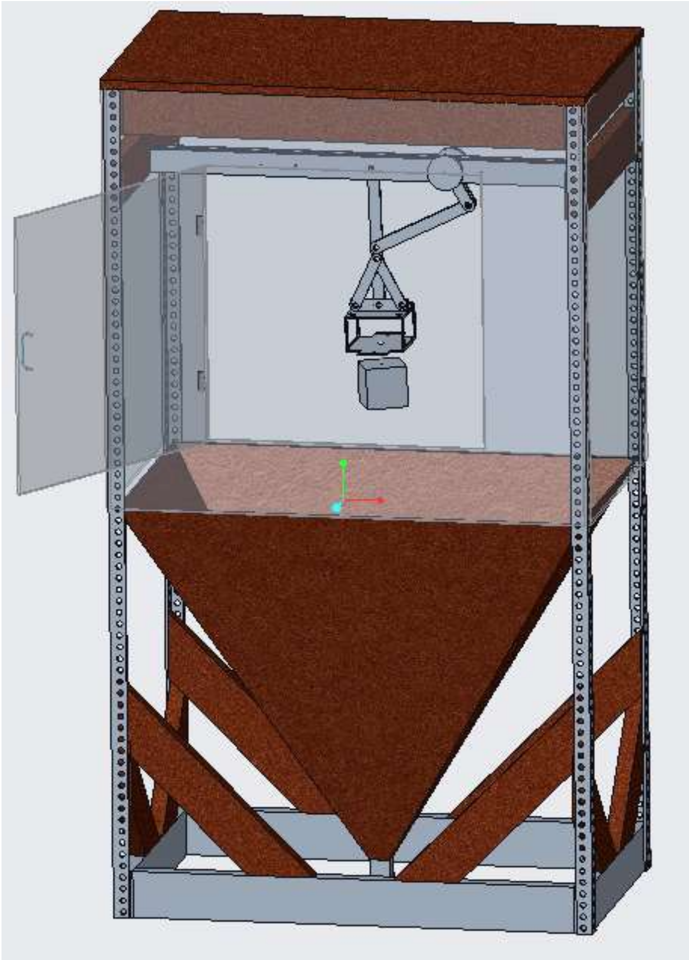

Figure 48 Final Design

Our prototype seen in Fig. 48 was successfully assembled according to our final model design. The final design is an ideal assembly, where the prototype had some minor differences in order minimize costs. The final design had four acrylic doors, where the final assembly incorporates two wooden walls. Also not pictured in the CAD drawings is the electrical components that are housed on top of the apparatus which provides a sturdy base to keep them away from the operator.

Figure 49 Full Mechanism Attached

Figure 50 Still Shots of Pendulum Motion

The working pendulum mechanism as demonstrated in Fig. 49 and Fig. 50, introduced the challenges during the building process. Keeping costs in mind, large gear ratios were utilized for the pendulum motion. This allowed our team to purchase less powerful motors, which are cheaper. This mechanism concept was actualized, but if the goals of the product were to change for handle heavier parts, swapping the motors would be only required adjustment. These motors were placed with ease of access in mind. Figure 51 shows the pendulum mechanism completely a full cycle. The pendulum sways 45 degrees on both sides without interference.

This test confirmed our initial design goals and calculations with the only change made being to move the motor mounts back in order to increase the tension of the belts to reduce slippage. After this the motors in the cage, used to rotate the build plate, were tested and functioned as intended spinning the shaft at the designated rotations per minute.

4.2 Build Challenges

Throughout the building process for this project, we faced several challenges in bringing it to fruition. One challenge was attaching the crank arms to the crank shaft of the pendulum. The original plan for these links was to create them from1/8-inch-thick aluminum stock and attach the link to the steel shaft via a press fit. The holes for a press fit must be precise, so they were machined using Esprit software on the Mini Mill. However, the steel shaft not only had a smaller diameter than listed by the manufacturer (the average diameter was slightly less than 0.374 inches) but its diameter was not constant down its length. The press fit holes were drilled with a diameter of 0.372 inches so that they could be adjusted if the hole was too small. When the shaft was pressed through the hole, the aluminum gave way to the steel due to its malleable nature and the thinness of the stock.

Since a press fit was not going to work, a new plan was devised to have a keyway in the links that would lock the crank arms in by creating a key slot within the shaft. This time a thicker stock material (0.25-inch-thick aluminum) was used. New holes were drilled, and the keyway was created using the EDM as explained in section 3.2. While the fix was somewhat simple, attaching these cranks took up a great deal of time due to unfamiliarity with Esprit and CNC machining as well as navigating Washburn labs, which were extremely booked up for a great deal of the term.

Another challenge that we have faced has come from 3D printing the parts we will use for testing the powder removal process. The impeller and the lattice cube have both failed printing twice. The problem has come from the thinness of the walls of the fins in the impeller as well as the walls of the cube. This issue has caused the walls to separate and not adhere correctly, blisters to develop along the thinnest faces of the parts, canceling of the prints part of the way through. We had tried recalibrating the extruder and readjusting the filament temperature, but the problems persisted. Careful process optimization should be performed to fabricate these complex geometries.

An additional challenge our team faced was the fact that we did not consider the width of the heads of the screw sleeves we were using as the joints between our links. This was a very simple fix as we just increased the distance between the three horizontal supports and added spacers where needed to accommodate this increased width.

We also originally wanted to use acrylic on all four sides so the user can see at every angle while the machine was in motion. However, this brought up some challenges because acrylic is very brittle and very hard to machine. Our sheets cracked while we were drilling the pilot holes for the bolts to mount it and the opening for the door. We then looked at our net cost and realized that it would be too much money to buy another sheet of acrylic and used the MDF panel board because of its low cost. This was a great substitute for the missing sides because it is less brittle, and easier to machine. This allowed us to mount the other sides easier without it cracking or breaking.

5. Recommendations

5.1 Final Assembly and Future Work

Final assembly of the prototype is to finish mounting the door and to completely seal the inside edge. The door assembly needs to be fully sealed and functional. The final part is to mount the 1’x1’ acrylic door to the mounted hinges on the MDF Panel board. Then align the inside of the door with the ½" gasket and attach the door handle and latch. This will then be a complete seal with the gasket acting as the sealant on the door frame. The way to seal the whole prototype is to use the same type of caulk we used to seal the chute system with. We would line every inside edge of the apparatus were the sides meet, the corners, the roof edge, and the edge between the chute and walls. This ensures that it will be completely sealed from the inside. This will help prevent any exterior air entering the prototype and disrupting the function. It will also prevent any of the loose powder to exit the prototype.

We were also working on a solution for the starting and stopping of our device, our team believes that a power switch to the motors is the best and simplest option as the Arduino would be able to run the code constantly and the operator can stop the device once the powder has been removed. Another idea is using our testing data to put a set number of steps the motors have to take in order to complete the cycle time. This will be slightly more work and require more research into programming the Arduino to accomplish this.

5.2 Test Procedure

First the geometry we will be testing in the device will be 3D printed. The first design we will test is a 2.67-inch lattice cube structure, which was created as shown below in Fig. 51. This lattice cube will be printed along with a 5” x 5” x1” base attached. This will act as the base plate that a part made through powder bed fusion would be fused to at the end of its printing process.

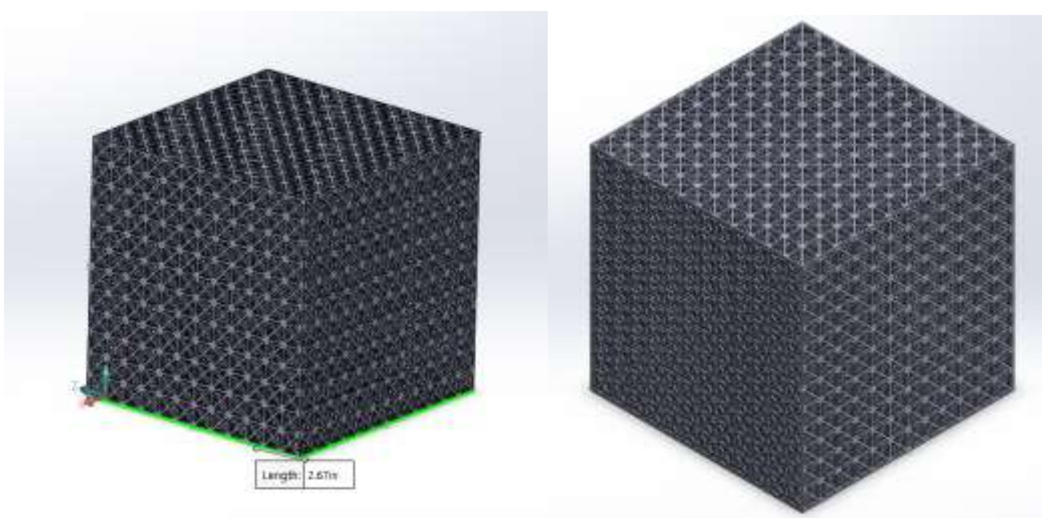

Figure 51 Lattice Cube

We will conduct the same tests on an impeller design with a diameter of 3.45 inches that is also fused to the same style 5” x 5” x 1” base plate attached seen in Fig. 52.

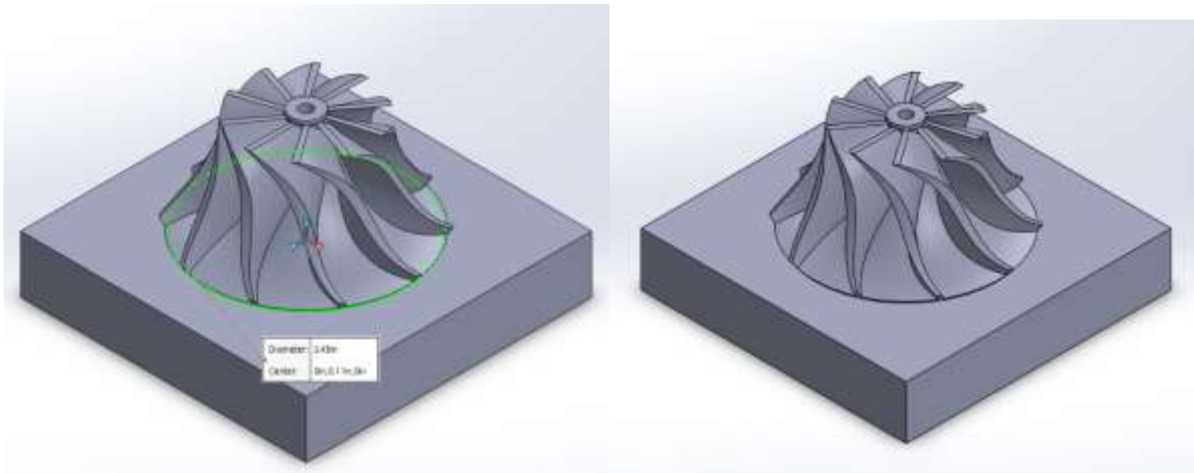

Figure 52 Impeller

The final test design will be done on a 3.94-inch-long helical gear as shown below in Fig. 53.

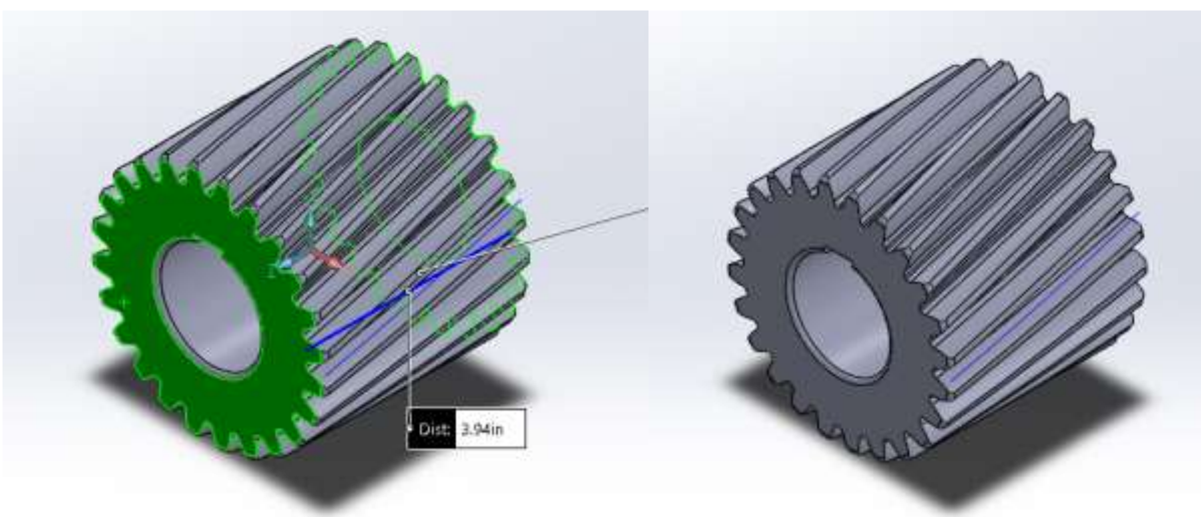

Figure 53 Helical Gear

Each 3D printed part will then be weighed twice, once without powder and once after being fully submerged in powder. At the end of the powder bed fusion process, the part is fully submerged in all the layers of powder it took to print. Fully engulfing the part in powder, taking care to ensure that the powder can get fully within the part, should offer the same effect. We will be using powdered sugar as our testing powder due to its particle size. The optimal particle size for LPBF is 15 - 45 microns and the optimal particle size for E-PBF is 45 - 106 microns. Out of several substances that we looked at including sand, flour, and several varieties of seasonings, powdered sugar (approximately 50 microns) came the closest to the correct particle size for both melting processes. The amount of initial powder at the start of testing will be dependent on the initial weight and final weight for each part that is used. The final weight after the powder removal process subtracted from the initial weight will give the amount of powder for each part. Each piece will then be mounted on to a plate that will be attached to the motors in the cage above to simulate the spinning motion. Figure 54 is included to demonstrate the relative particle size of various materials.

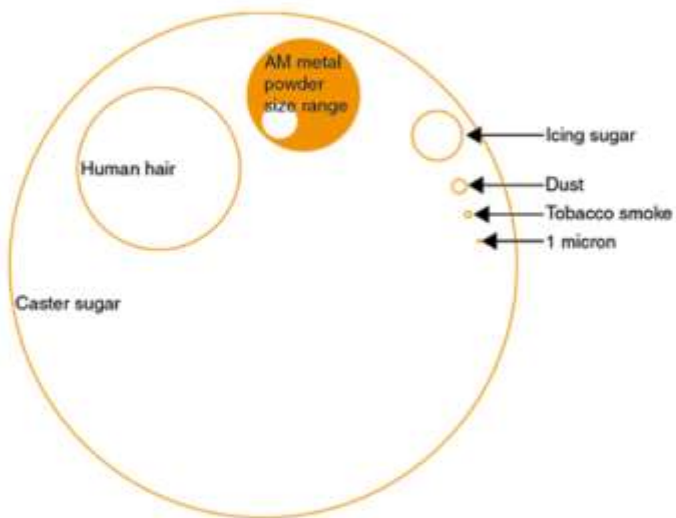

Figure 54 Particle Size Comparison Image Credit: (Reinshaw)

The first test's objective is to determine if all the powder can be removed from the part using the device. The speed of each of the four motors will be set to1 RPM at the start and adjusted based on how they perform once the base is attached. The revolutions per minute of each stepper motor can be calculated by the number of steps per second divided by the steps per revolution multiplied by 60 seconds.

$$\frac{60(steps\ per\ second)}{steps\ per\ revolution} = revolutions\ per\ second$$

For example, if the Arduino code is set at 300 steps per revolution at a rate of 30 steps per second the resulting speed would be 6 RPM. The results of this test will be recorded in the table below, along with the speed of each motor, the time passed at each inspection interval, the number of passes the pendulum has taken from each most extreme angle, the weight at the beginning and end of each interval, and the percentage of powder removed from the part at each time interval.

Efficiency Test

Speed of Motor 1 (RPM)	Speed of Motor 2 (RPM)	Speed of Motor 3 (RPM)	Speed of Motor 4 (RPM)	Time Interval (s)	# of Passes	Initial Weight (g)	Final Weight (g)	Percentage of Powder Removed
				60				
				120				
				180				
				240				

The next evaluation we will conduct is a speed test, which will measure how fast the machine can remove powder from each part. We will do four trials and increase the motor speed each time, calculated in revolutions per minute. The first trial will be done at the rate of our first test of efficiency, which will be done slowly at 1 RPM. For the successive tests, we will increase the speed by 2 RPMs for each trial. We may adjust the speeds of the first two motors working the pendulum differently from the second two spinning the base plate contingent upon the outcomes of the efficiency test. The results of these trials will be recorded in the table below with the speeds of each motor, the initial and final weights, the percentage of powder removal, and the time.

Speed Test for Powder Removal

Trial #	Speed of Motor 1 (RPM)	Speed of Motor 2 (RPM)	Speed of Motor 3 (RPM)	Speed of Motor 4 (RPM)	Initial Weight (g)	Final Weight (g)	Percentage of Powder Removed	Time (s)
1	1	1						
2	3	3						
3	5	5						
4	7	7						

References

A Consideration of EBM versus DMLS Industrial Metal 3D Printing Processes, Part 1. (2016). Retrieved September 23, 2019, from https://www.fabbaloo.com/blog/2016/4/17/a-consideration-of-ebm-versus-dmls-industrial-metal-3d-printing-processes-part-1

Additive Manufacturing: Overcoming Current Limitations. (2018). Retrieved September 30, 2019, from https://www.pivotint.com/blog/additive-manufacturing-overcoming-current-limitations

Atkinson, H. v., & Davies, S. (2000). Fundamental aspects of hot isostatic pressing: An overview. *Metallurgical and Materials Transactions A: Physical Metallurgy and Materials Science, 31*(12), 2981–3000. https://doi.org/10.1007/s11661-000-0078-2

Bhavar, V., Kattire, P., Patil, V., Khot, S., Gujar, K., & Singh, R. (2017). A review on powder bed fusion technology of metal additive manufacturing. In *Additive Manufacturing Handbook* (pp. 251–253). https://doi.org/10.1201/9781315119106-15

Bonini, J., Mazza, K. C., Morra, J. (2016). Cleanliness and Microstructural Issues Related to Additive Layer Manufactured Porous Surface Structured Titanium Medical and Dental Implants. Proceedings of the 13th World Conference on Titanium, 1751-1759. doi:10.1002/9781119296126.ch295

Direct Metal Laser Sintering | 3D Printing | Protolabs. Retrieved September 25, 2019, from https://www.protolabs.com/services/3d-printing/direct-metal-laser-sintering/

Direct Metal Laser Sintering | DMLS | Metal 3D Printing. Retrieved September 23, 2019, from https://www.xometry.com/direct-metal-laser-sintering?ads_cmpid=1726562607&ads_adid=66555601574&ads_matchtype=b&ads_network=g&ads_creative=336742797982&utm_term=%2Bdmls&ads_targetid=kwd-51790985356&utm_campaign=&utm_source=google&utm_medium=cpc&ttv=2&gclid

Direct Metal Laser Sintering - an overview | ScienceDirect Topics. (2014). Retrieved September 25, 2019, from https://www.sciencedirect.com/topics/materials-science/direct-metal-laser-sintering

Direct Metal Laser Sintering (DMLS) – Simply Explained | All3DP. (2019). Retrieved September 25, 2019, from https://all3dp.com/2/direct-metal-laser-sintering-dmls-simply-explained/

Direct Metal Laser Sintering [DMLS] Parts On Demand. Retrieved September 23, 2019, from https://www.stratasysdirect.com/technologies/direct-metal-laser-sintering#dmls-materials

DMLS Applications. Retrieved September 25, 2019, from https://dmlstechnology.com/dmls-applications

DMLS: Understanding Additive Metal Manufacturing | Stratasys Direct. Retrieved September 23, 2019, from https://www.stratasysdirect.com/technologies/direct-metal-laser-sintering/dmls-understanding-additive-metal-manufacturing

Dong, G., Marleau-Finley, J., & Zhao, Y. F. (2019). Investigation of electrochemical post-processing procedure for Ti-6Al-4V lattice structure manufactured by direct metal laser sintering (DMLS). *International Journal of Advanced Manufacturing Technology*. https://doi.org/10.1007/s00170-019-03996-5

Drescher, P., Reimann, T., & Seitz, H. (2014). Investigation of powder removal of net-structured titanium parts made from electron beam melting. *International Journal of Rapid Manufacturing*, *4*(2/3/4), 81. https://doi.org/10.1504/ijrapidm.2014.066007

Electron Beam Melting - EBM Process, Additive Manufacturing | Arcam AB. Retrieved September 23, 2019, from http://www.arcam.com/technology/electron-beam-melting/

Electron Beam Melting Machines | EBM Machines | GE Additive. Retrieved September 23, 2019, from https://www.ge.com/additive/additive-manufacturing/machines/ebm-machines

First titanium 3D-printed part installed into serial production aircraft - Commercial Aircraft - Airbus. (2017). Retrieved October 6, 2019, from https://www.airbus.com/newsroom/press-releases/en/2017/09/first-titanium-3d-printed-part-installed-into-serial-production-.html

Ford, S., & Despeisse, M. (2016). Additive manufacturing and sustainability: an exploratory study of the advantages and challenges. *Journal of Cleaner Production*, *137*, 1573–1587. https://doi.org/10.1016/j.jclepro.2016.04.150

Gibson, I., Rosen, D. W., & Stucker, B. (2010). Design for Additive Manufacturing. Additive Manufacturing Technologies, 299–332. doi: 10.1007/978-1-4419-1120-9_11

GM's Use of 3-D Printing Predicts Cheaper, Better Cars | WIRED. (2018). Retrieved October 6, 2019, from https://www.wired.com/story/general-motors-auto-industry-3d-printing-additive-manufacturing/

Gradl, P. R., Greene, S. E., Protz, C., Bullard, B., Buzzell, J., Garcia, C., . . . Cooper, K. G. (2018). Additive Manufacturing of Liquid Rocket Engine Combustion Devices: A Summary of Process Developments and Hot-Fire Testing Results. 2018 Joint Propulsion Conference. doi:10.2514/6.2018-4625

Hamzah, N. A., Mohd Tamrin, S. B., & Ismail, N. H. (2016). Metal dust exposure and lung function deterioration among steel workers: an exposure-response relationship. *International Journal of Occupational and Environmental Health*, *22*(3), 224–232. https://doi.org/10.1080/10773525.2016.1207040

Herderick, E. D. (2015). Progress in Additive Manufacturing. Jom, 67(3), 580–581. doi: 10.1007/s11837-015-1323-x

How Direct Metal Laser Sintering (DMLS) Really Works | 3D Printing Blog | i.materialise. (2019). Retrieved September 25, 2019, from https://i.materialise.com/blog/en/direct-metal-laser-sintering-dmls/

Manufacturing. BusinessDictionary.com. Retrieved May 03, 2020, from BusinessDictionary.com website: http://www.businessdictionary.com/definition/manufacturing.html

Marshall, George C. National Aeronautics and Space Administration. Retrieved October 6, 2019. website: www.nasa.gov

Mehrjerdi, Y. Z. (2011). Six-Sigma: methodology, tools and its future. Assembly Automation, 31(1), 79–88. doi: 10.1108/01445151111104209

NFPA 484: Standard for Combustible Metals. Retrieved September 30, 2019, from https://www.nfpa.org/codes-and-standards/all-codes-and-standards/list-of-codes-and-standards/detail?code=484

Powder bed fusion - DMLS, SLS, SLM, MJF, EBM | Make. Retrieved September 23, 2019, from https://make.3dexperience.3ds.com/processes/powder-bed-fusion

Pouspourika, K. (2019, June 30). The 4 Industrial Revolutions. Retrieved from https://ied.eu/project-updates/the-4-industrial-revolutions/

Renishaw. Metal powders for AM. Retrieved March 5, 2020, from https://www.renishaw.com/en/metal-powders-for-am--31457

Rolls-Royce to Fly Large 3D Printed Part - 3D Printing Industry. (2015). Retrieved October 6, 2019, from https://3dprintingindustry.com/news/rolls-royce-to-fly-largest-3d-printed-part-ever-flown-42795/

Scime, L., Wolf, S. D. V., Beuth, J., Mrdjenovich, S., & Kelley, M. (2018). Safety and Workflow Considerations for Modern Metal Additive Manufacturing Facilities. *JOM*, *70*(9), 1830–1834. https://doi.org/10.1007/s11837-018-2971-4

Tan, K. L., & Yeo, S. H. (2017). Surface modification of additive manufactured components by ultrasonic cavitation abrasive finishing. *Wear*, *378–379*, 90–95. https://doi.org/10.1016/j.wear.2017.02.030

Tay, F. E. H., & Haider, E. A. (2002). Laser sintered rapid tools with improved surface finish and strength using plating technology. *Journal of Materials Processing Technology*, *121*(2–3), 318–322. https://doi.org/10.1016/S0924-0136(01)01220-1

The limitation of the Additive Manufacturing (3D Printing). (2017). Retrieved September 30, 2019, from https://medium.com/@CoCoCool_SS/the-limitation-of-the-additive-manufacturing-3d-printing-7b6ff7df521f

Wohlers, T., & Gornet, T. (2016). *History of Additive Manufacturing*.

Appendices

Appendix A. Project Interview Questions

2019-2020 WPI Powder Cleaning Apparatus Major Qualifying Project Interview Questions

Thank you for taking the time to answer our questions.

Our project team believes that this survey will take approximately 5-10 minutes

These questions are aimed to focus this project group's scope to the key issues and design constraints with powder removal of from parts fabricated using laser powder bed fusion additive manufacturing. Our project team aims to create a prototype for an apparatus that can remove the residual powder from small scale additively manufactured parts. This is a year-long major qualifying project (senior design project), so the goal of this team is not to create commercial grade apparatus but rather to understand and identify the fundamental issues with the process and create a prototype to address those issues.

Name (optional):

Please state your experience level with additive manufacturing (# of years in field):

1) What is your current involvement within this field and what type(s) of additive manufacturing do you currently work with?

2) Do you have hands on experience with setting up, running, or with post processing powder bed fusion parts?

3) Without divulging any export controlled or proprietary information, how does your company or research lab remove loose powder from metal additively manufactured parts?

4) What are the some of the biggest challenges you face with metal powder removal?

5) Are there any other key issues that our project team should investigate regarding powder removal?

Appendix B. Summary of Project Interview Questions

2019-2020 WPI Powder Cleaning Apparatus Major Qualifying Project Interview Questions

Thank you for taking the time to answer our questions.

Our project team believes that this survey will take approximately 5-10 minutes

These questions are aimed to focus this project group's scope to the key issues and design constraints with powder removal of from parts fabricated using laser powder bed fusion additive manufacturing. Our project team aims to create a prototype for an apparatus that can remove the residual powder from small scale additively manufactured parts. This is a year-long major qualifying project (senior design project), so the goal of this team is not to create commercial grade apparatus but rather to understand and identify the fundamental issues with the process and create a prototype to address those issues.

Name (optional):

Our project team has removed the names of the participants but we received six responses from professionals within the field of additive manufacturing.

Please state your experience level with additive manufacturing (# of years in field):

Our participants had experience ranging from two to fifteen years of experience in this field.

1) What is your current involvement within this field and what type(s) of additive manufacturing do you currently work with?

Our participants included both lab researchers and commercial production managers. In addition to this there was a wide range of machine and process types that included polymer and metal powder based systems. These participants also work with both reactive and non-reactive powders.

2) Do you have hands on experience with setting up, running, or with post processing powder bed fusion parts?

All of our participants had experience with these processes.

3) Without divulging any export controlled or proprietary information, how does your company or research lab remove loose powder from metal additively manufactured parts?

This generally involved a substantial amount of manual labor with brushing or chiseling off caked on powder in the case of electron beam melting, in a few cases some participants had small, handmade devices that added a vibration. There was one case where a percipient used a commercial available unit that again utilized vibrations to aid in powder removal.

4) What are the some of the biggest challenges you face with metal powder removal?

Two of the biggest challenges our participants stated were removing powder from intricate or internal features, especially if the internal powder is partially sintered, and ensuring recovered powder is not contaminated.

5) Are there any other key issues that our project team should investigate regarding powder removal?

One big concern was the effect of vibrations on the part in question and if that had any long lasting effect on the structural integrity of the parts. Another concern was a method to verify that all of the residual powder had been removed.